



# First analysis of Belle II energy scan data

Qingping Ji (Henan Normal University)

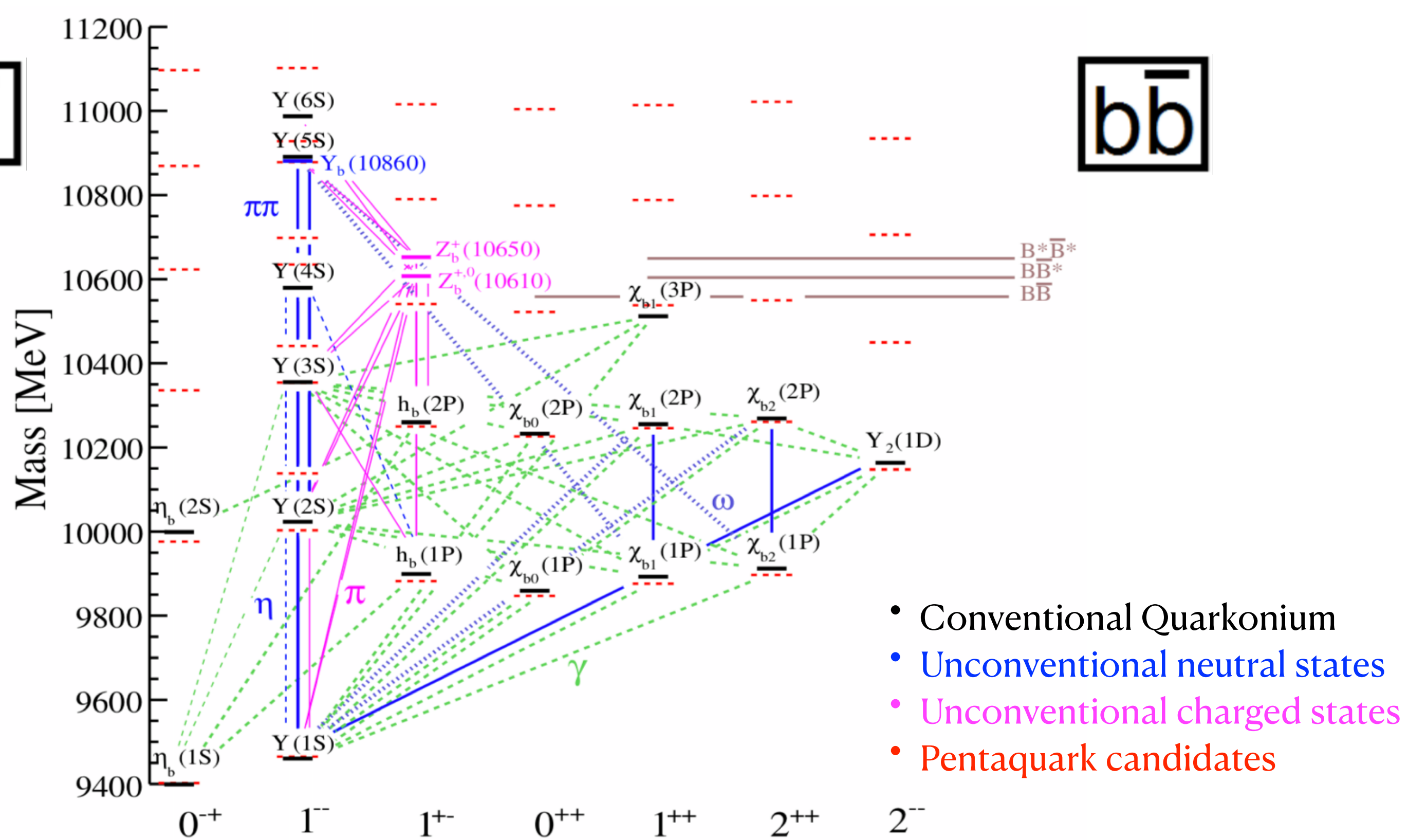
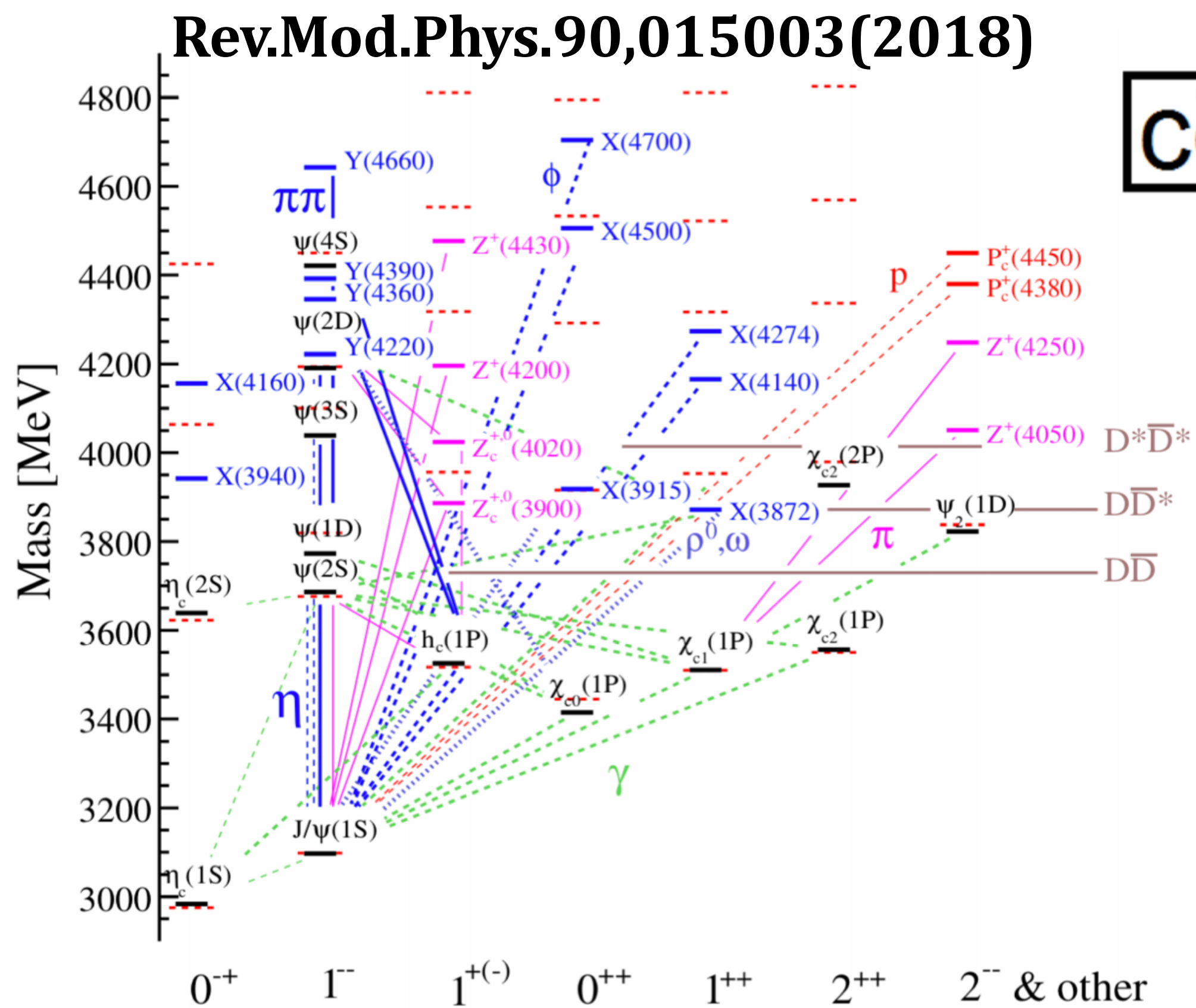
( On behalf of the Belle II Collaboration )



ICHEP 2022  
BOLOGNA

ICHEP 2022  
XLI  
International Conference  
on High Energy Physics  
Bologna (Italy)

# Quarkonium



- Conventional Quarkonium
- Unconventional neutral states
- Unconventional charged states
- Pentaquark candidates

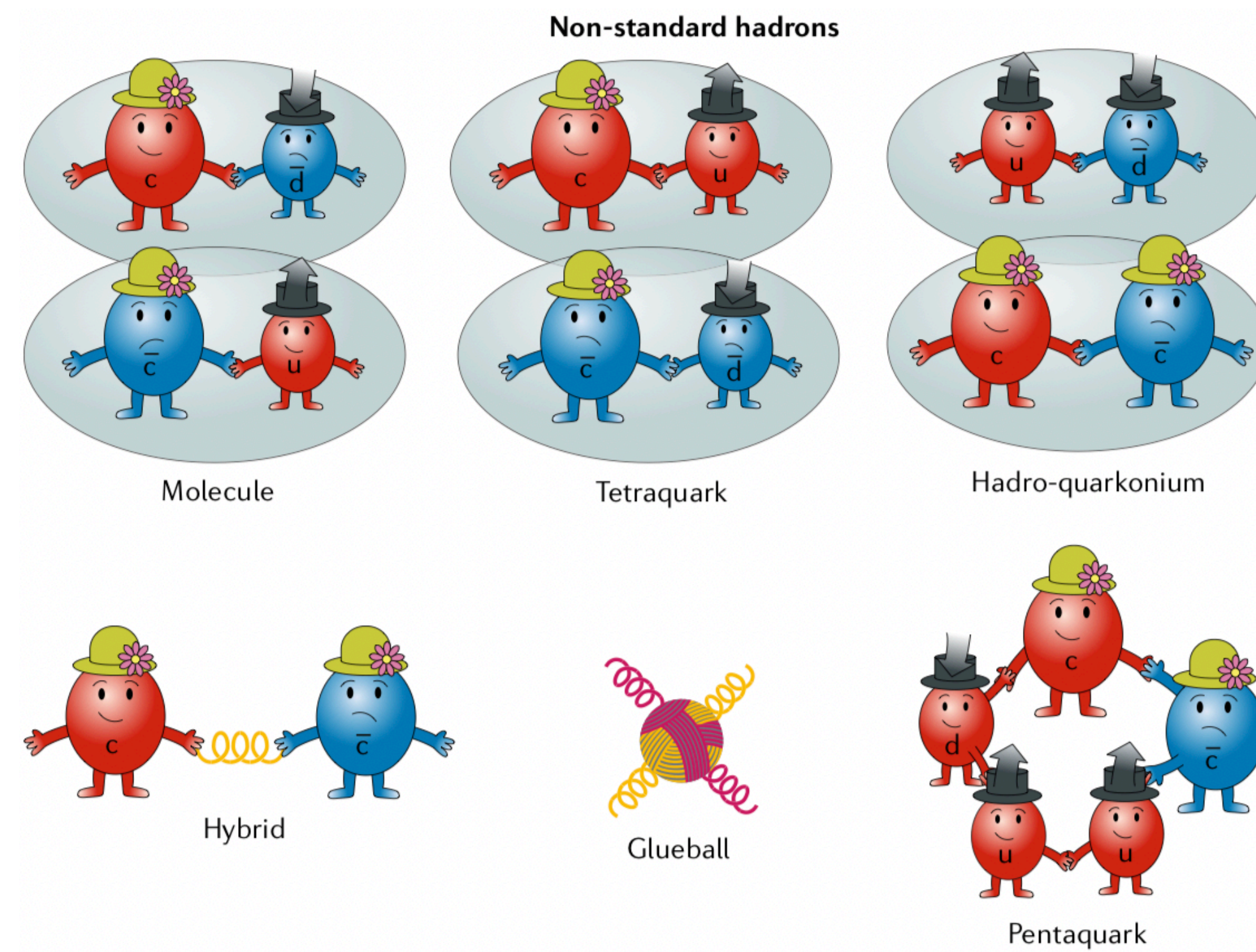
- Below  $D\bar{D}/B\bar{B}$  thresholds-both charmonium and bottomonium are successful stories of QCD.
- There are certain parallels in the properties of hadrons containing  $c\bar{c}$  and  $b\bar{b}$ .



# Exotic interpretations

Quark model [Physics Letters 8, 214(1964)]:

- Conventional hadrons: mesons (2 quarks) and baryons (3 quarks)
- QCD does not forbid hadrons with  $> 3$  quarks !!



Nature Rev. Phys. 1(2019)8, 480-494 (2019)

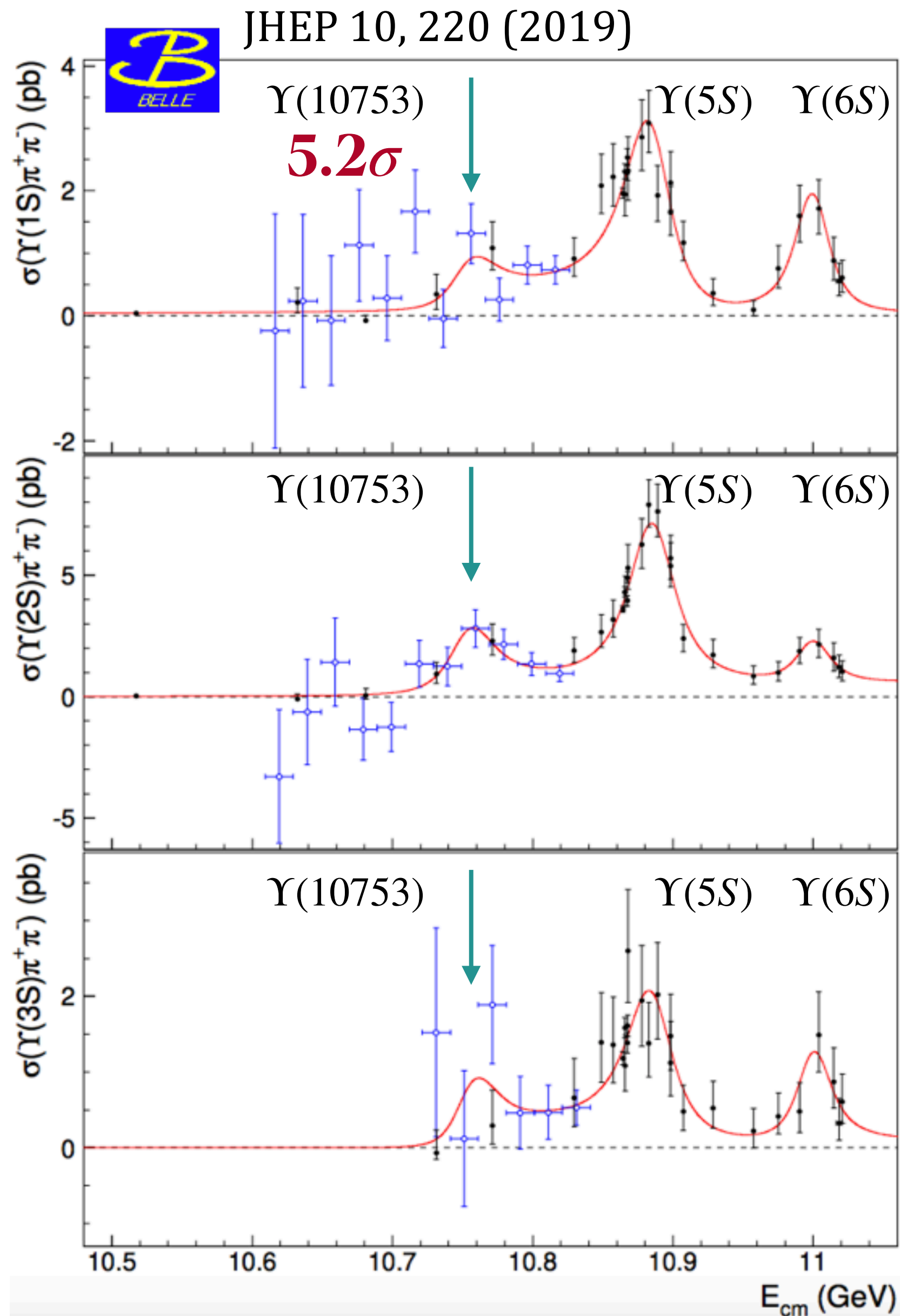
Physics Reports 873,1 (2020)

In addition, screened potential, cusps effect, final state interaction ...

**High priority: seek unified picture describing all XYZ states, not state-by-state**



# New structure: $\Upsilon(10753)$



- Belle: several  $\sim 1\text{fb}^{-1}$  scan points below  $\Upsilon(5S)$
- New structure  $\Upsilon(10753)$  observed in the  $\pi^+\pi^-\Upsilon(nS)$  transition<sup>[1]</sup>

|                         | $\Upsilon(10860)$                    | $\Upsilon(11020)$                       | New structure                          |
|-------------------------|--------------------------------------|---|--|
| M (MeV/c <sup>2</sup> ) | $10885.3 \pm 1.5^{+2.2}_{-0.9}$      | $11000.0^{+4.0}_{-4.5}{}^{+1.0}_{-1.3}$ | $10752.7 \pm 5.9^{+0.7}_{-1.1}$        |
| $\Gamma$ (MeV)          | $36.6^{+4.5}_{-3.9}{}^{+0.5}_{-1.1}$ | $23.8^{+8.0}_{-6.8}{}^{+0.7}_{-1.8}$    | $35.5^{+17.6}_{-11.3}{}^{+3.9}_{-3.3}$ |

- Interpreted as conventional bottomonium<sup>[2]</sup> or exotics state<sup>[3]</sup>.
- Predicted to decay into  $\omega\chi_{bJ}$  with a BF of  $10^{-3}$  based on the mixing of conventional states 4S and 3D<sup>[4]</sup>.

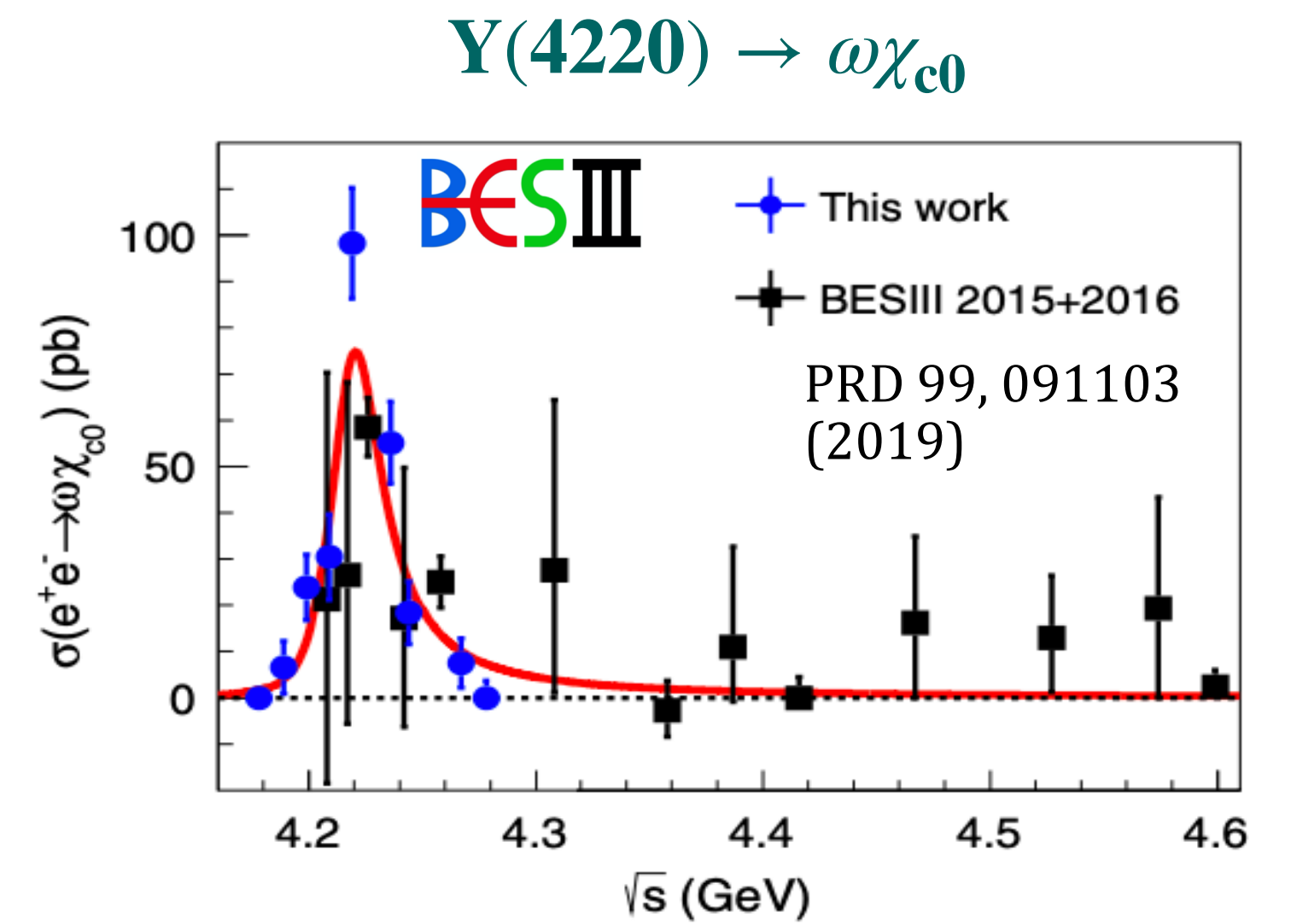
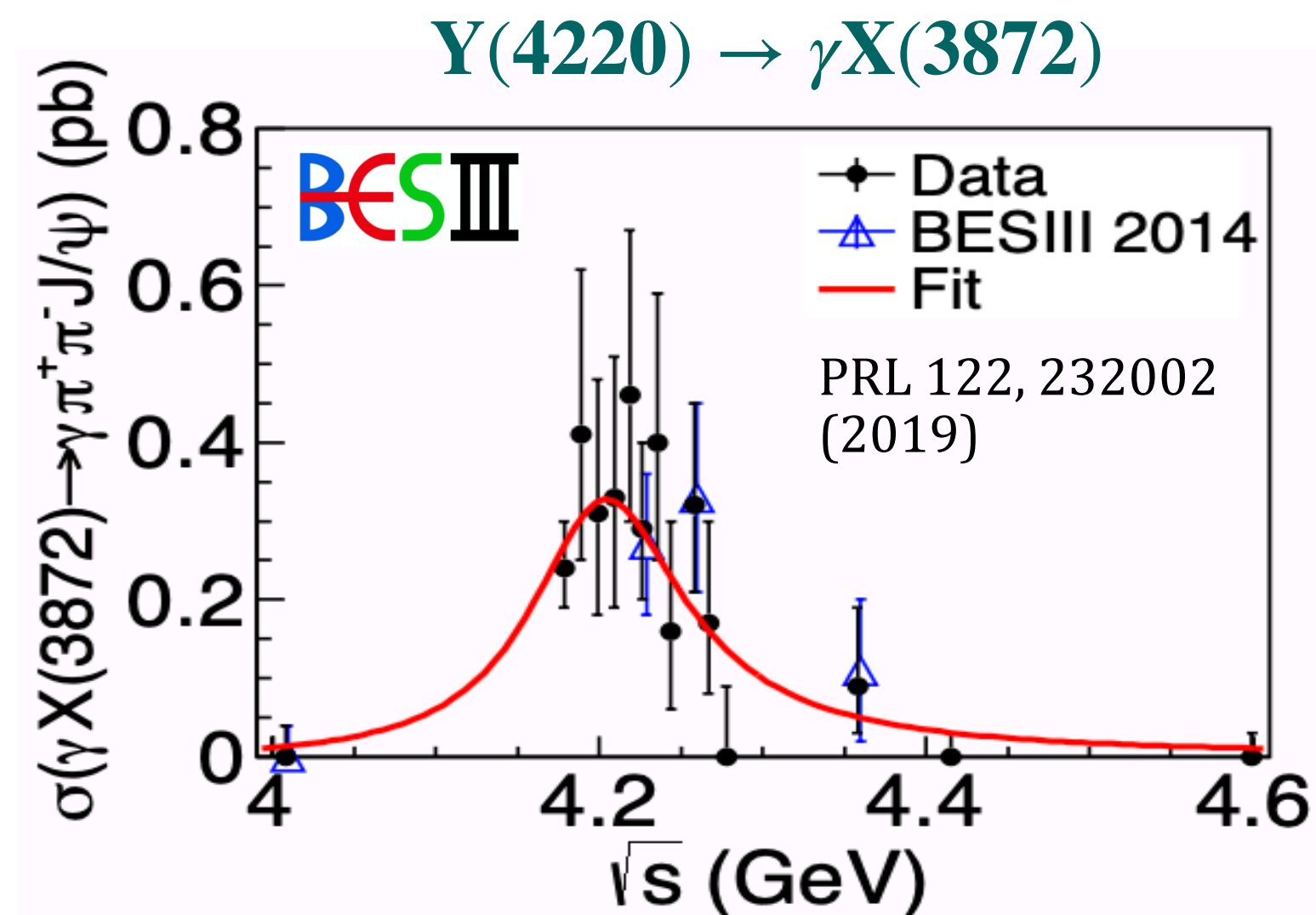
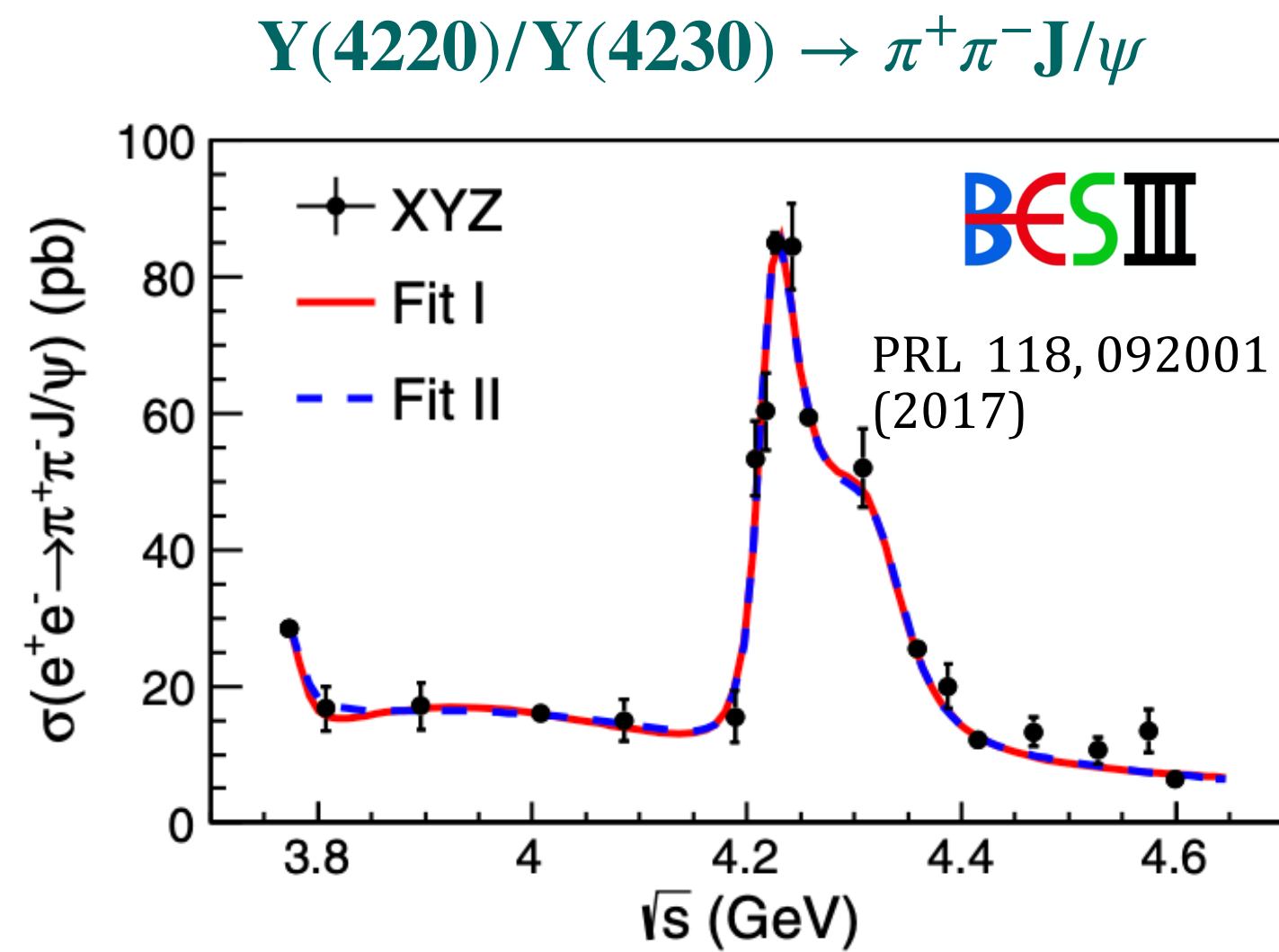
[1]. JHEP 10, 220 (2019); [2]. PRD 105, 074007(2022); PRD 104,034036 (2021); EPJC 80,59 (2020)

[3]. PRD 104,034019(2021); PRD 103,074507(2021); Chin. Phys. C 43, 123102 (2019); [4]. PRD 104,034036(2021).



# $X_b$ : Bottomonium counterpart of $X(3872)$ ?

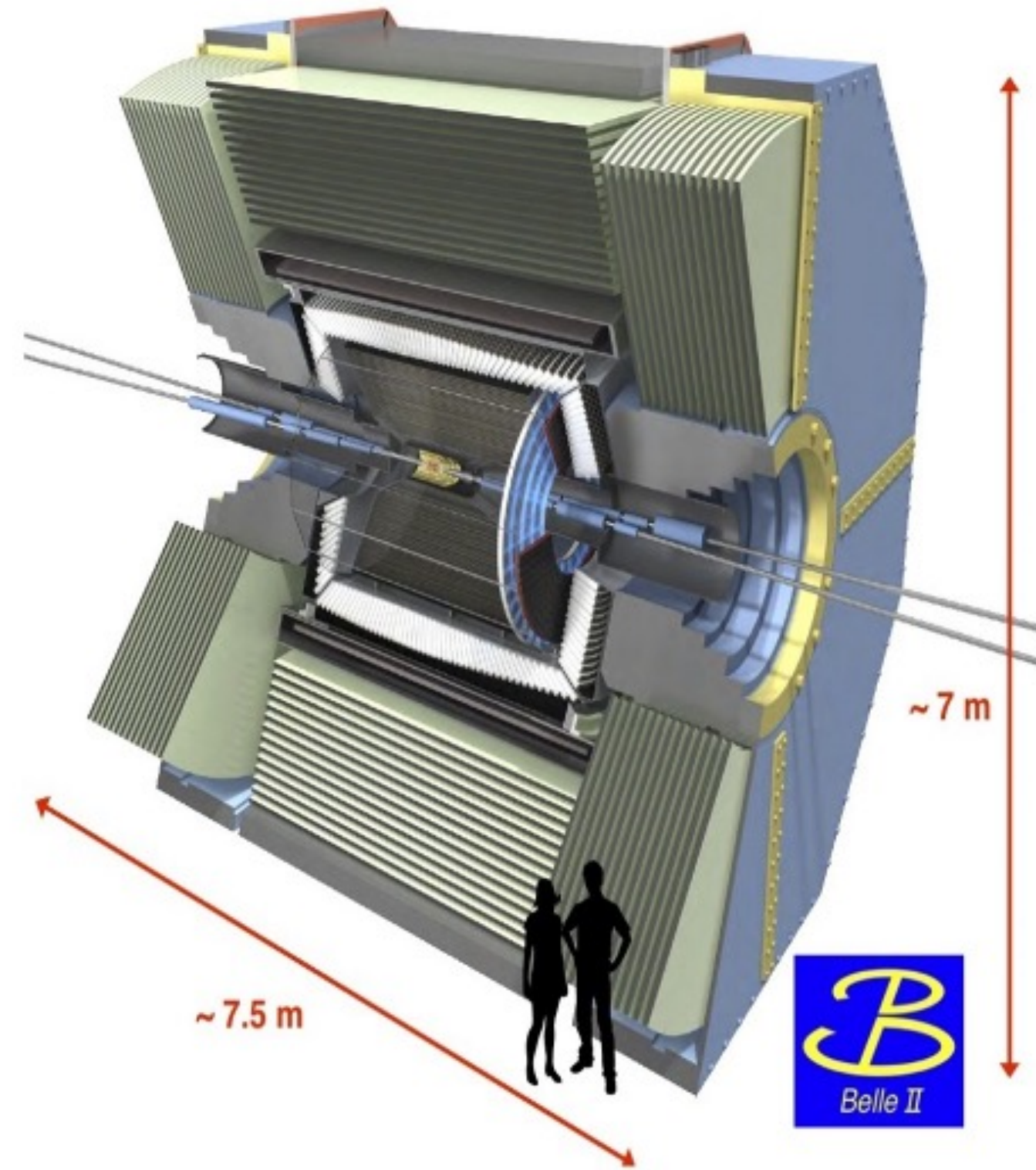
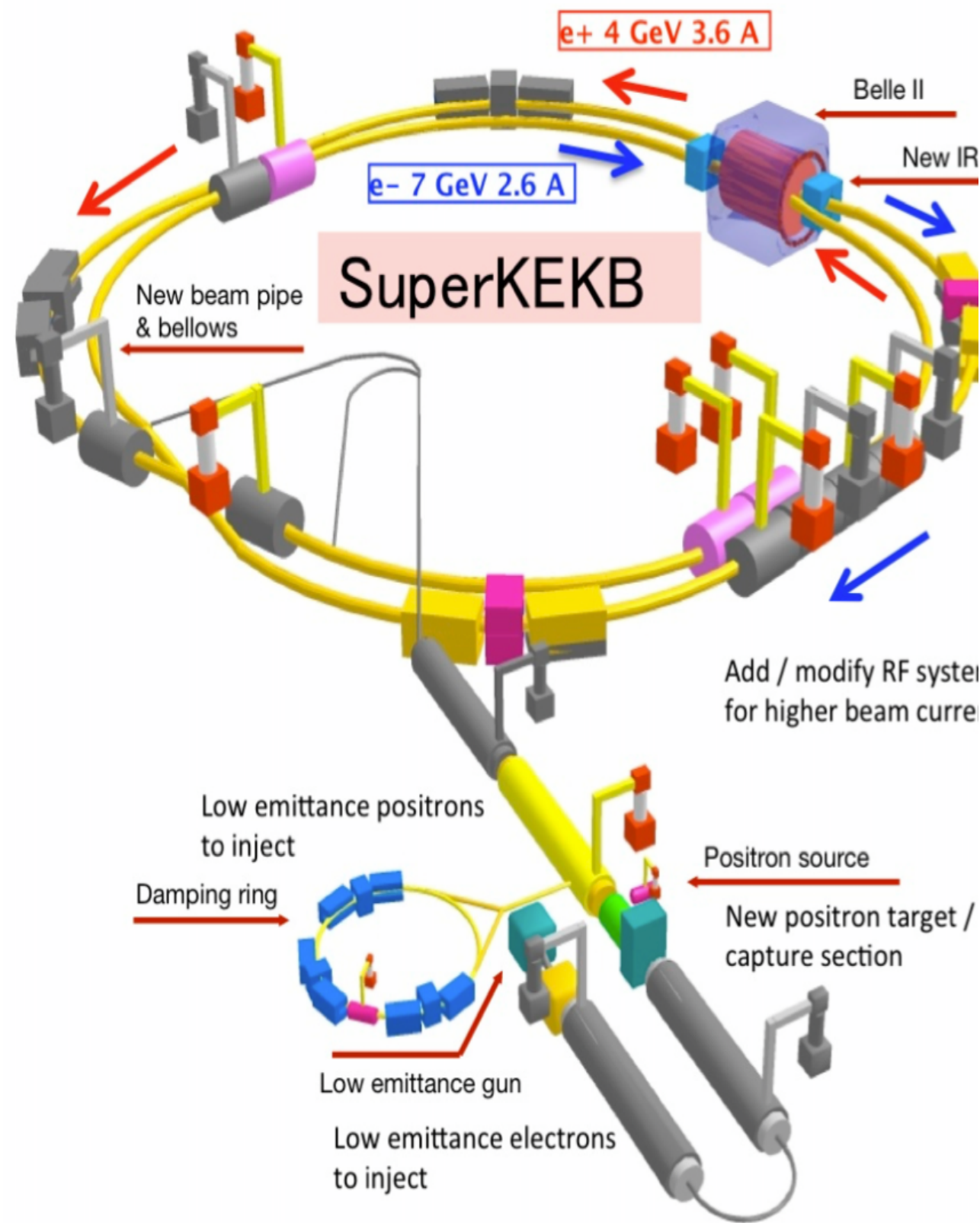
- Two close peaks observed in the cross sections for  $e^+e^- \rightarrow \pi^+\pi^-J/\psi$  by BESIII<sup>[1]</sup> and  $e^+e^- \rightarrow \pi^+\pi^-\Upsilon(nS)$  by Belle<sup>[2]</sup>, respectively. These peaks may indicate similar nature.
- $Y(4220) \rightarrow \gamma X(3872)$ <sup>[3]</sup> and  $\omega\chi_{c0}$ <sup>[4]</sup>, observed by BESIII.
- Evidence of  $\Upsilon(5S) \rightarrow \omega\chi_{b1,2}$  observed by Belle<sup>[5]</sup>, BESIII observed higher charmonium decays to  $\omega\chi_{c1,2}$ <sup>[6]</sup>.
- So expect the  $\Upsilon(10753)$  state to decay into  $\gamma X_b$  with  $X_b \rightarrow \omega\Upsilon(1S)$ , as well as a potential resonance in the line shape of  $\sigma(e^+e^- \rightarrow \omega\chi_{b1,2})$ .



[1]. PRL 91, 262001(2003); [2]. JHEP 10, 220 (2019); [3]. PRL 122, 232002 (2019); [4]. PRD 99, 091103 (2019); [5]. PRD 98, 091102 (2018); [6]. PRD 93,011102(R) (2016)



# SuperKEKB and Belle II capabilities

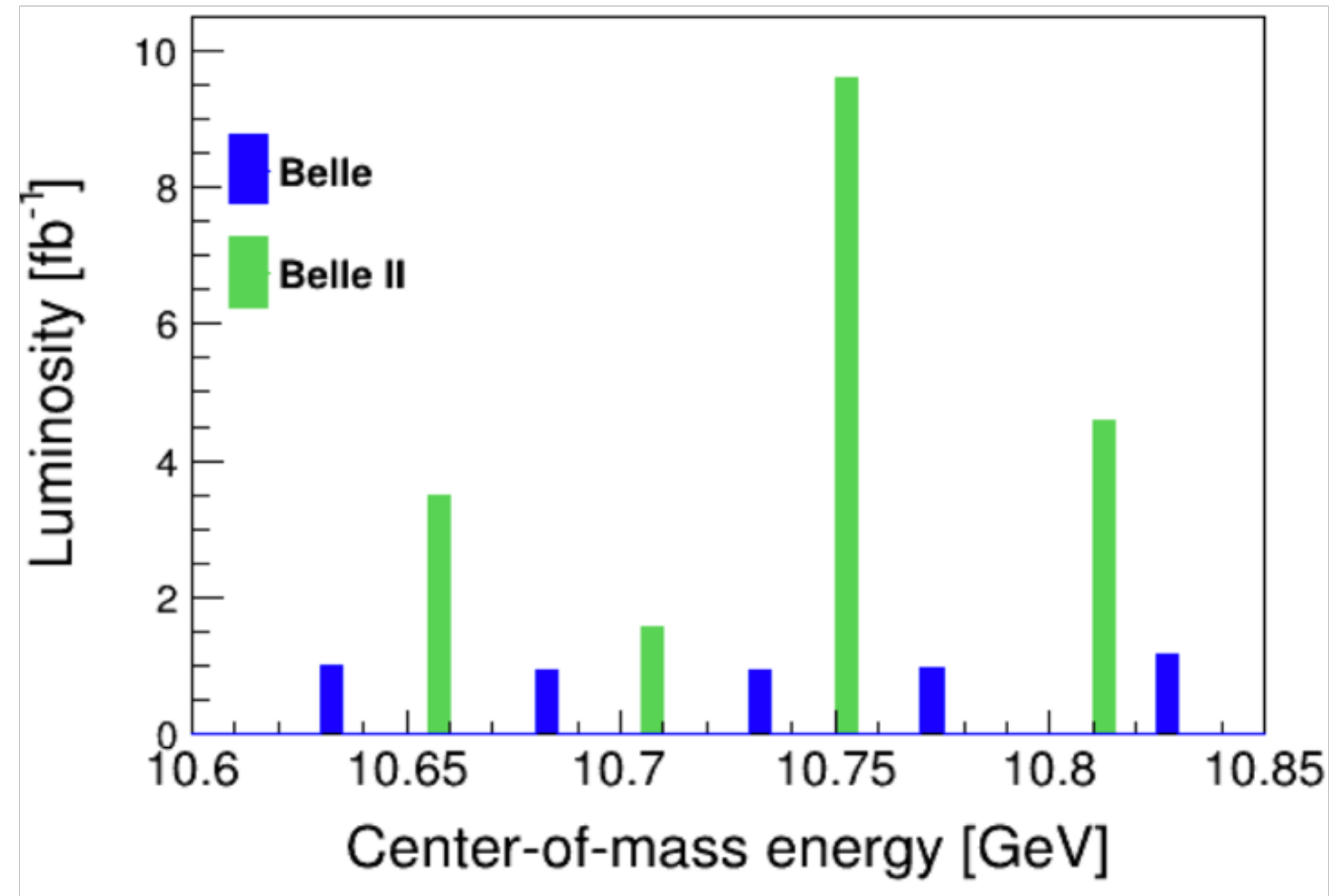


- Asymmetric energy  $e^+e^-$  (4 & 7 GeV) collider in Tsukuba, Japan
- Much higher luminosity than predecessor
- Upgraded detectors (better vertex and particle identification performances)
- Achieved peak luminosity:  $4.7 \times 10^{34} \text{ cm}^2 \text{ s}^{-1}$
- Integrated luminosity:  $\sim 424 / \text{fb}$ .



# Unique scan data near $\sqrt{s} = 10.75 \text{ GeV}$

- In November 2021, Belle II collected  $19\text{fb}^{-1}$  of unique data at energies above the  $\Upsilon(4S)$ : four energy scan points around 10.75 GeV
- Physics goal: understand the nature of the  $\Upsilon(10753)$  energy region.



This is the first showing of these results.

# Analysis goals

$$e^+e^- \rightarrow \omega\chi_{bJ}:$$

- Determine the Born cross section for  $e^+e^- \rightarrow \omega\chi_{bJ}$  using unique scan data samples at  $\sqrt{s} = 10.701, 10.745$  and  $10.805$  GeV.
- Study the energy dependence cross section of  $e^+e^- \rightarrow \omega\chi_{bJ}$ , by combining with Belle data at  $\sqrt{s} = 10.867$  GeV<sup>[1]</sup>.

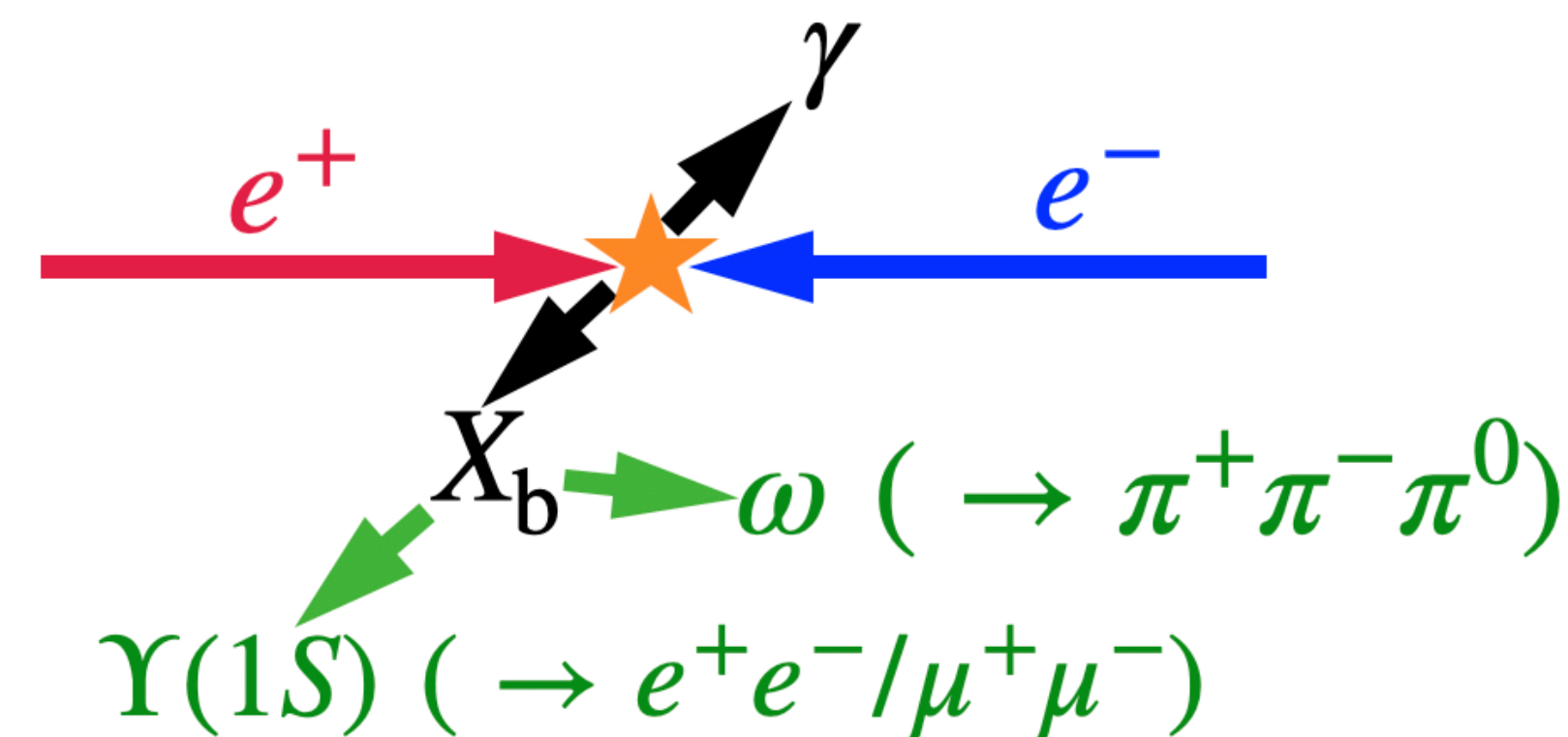
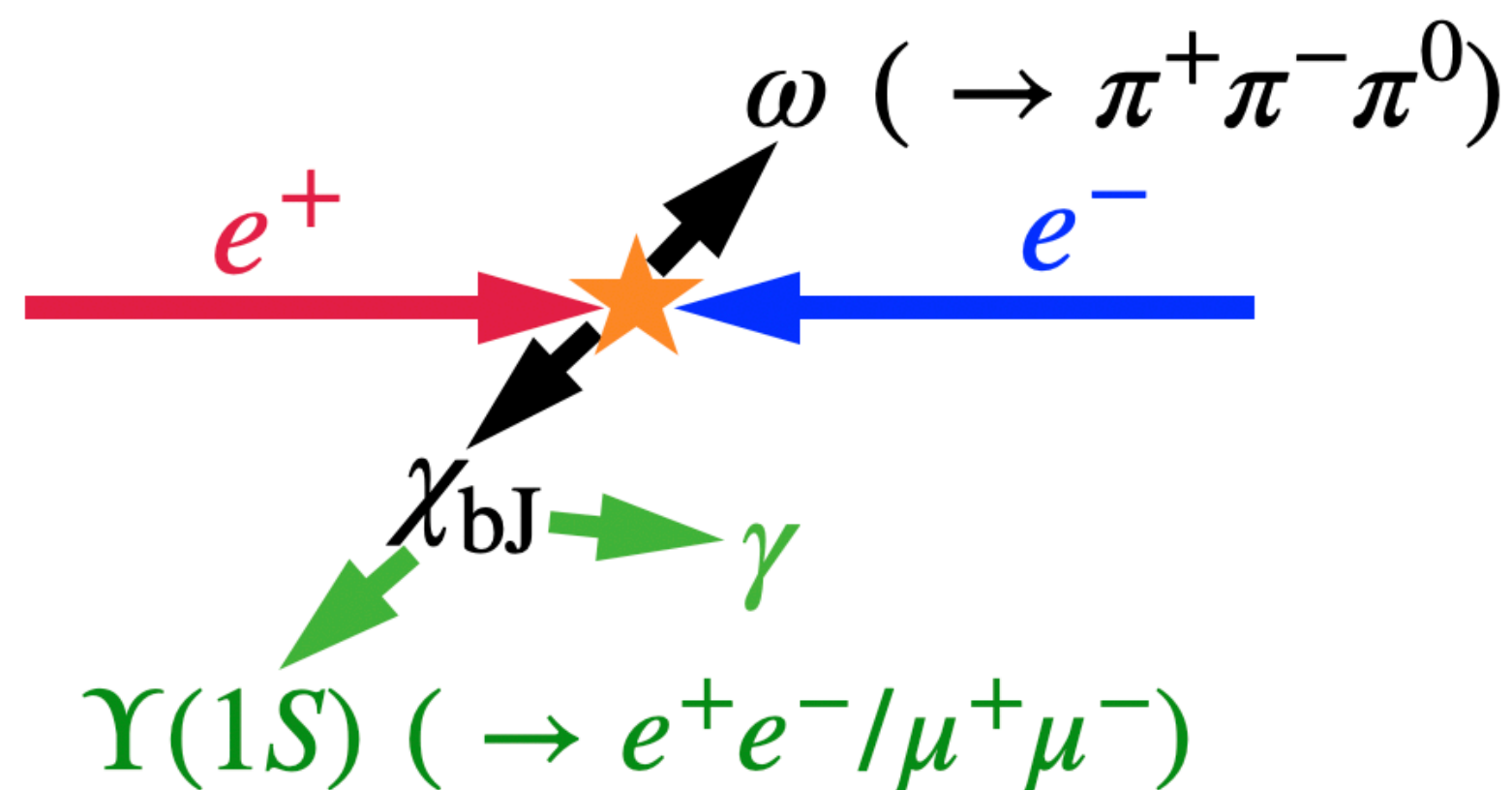
$$e^+e^- \rightarrow \gamma X_b:$$

- Search for the  $X_b$  using the unique scan data samples at  $\sqrt{s} = 10.645, 10.701, 10.745$  and  $10.805$  GeV

[1]PRL 113, 142001(2014);



# Analysis overview

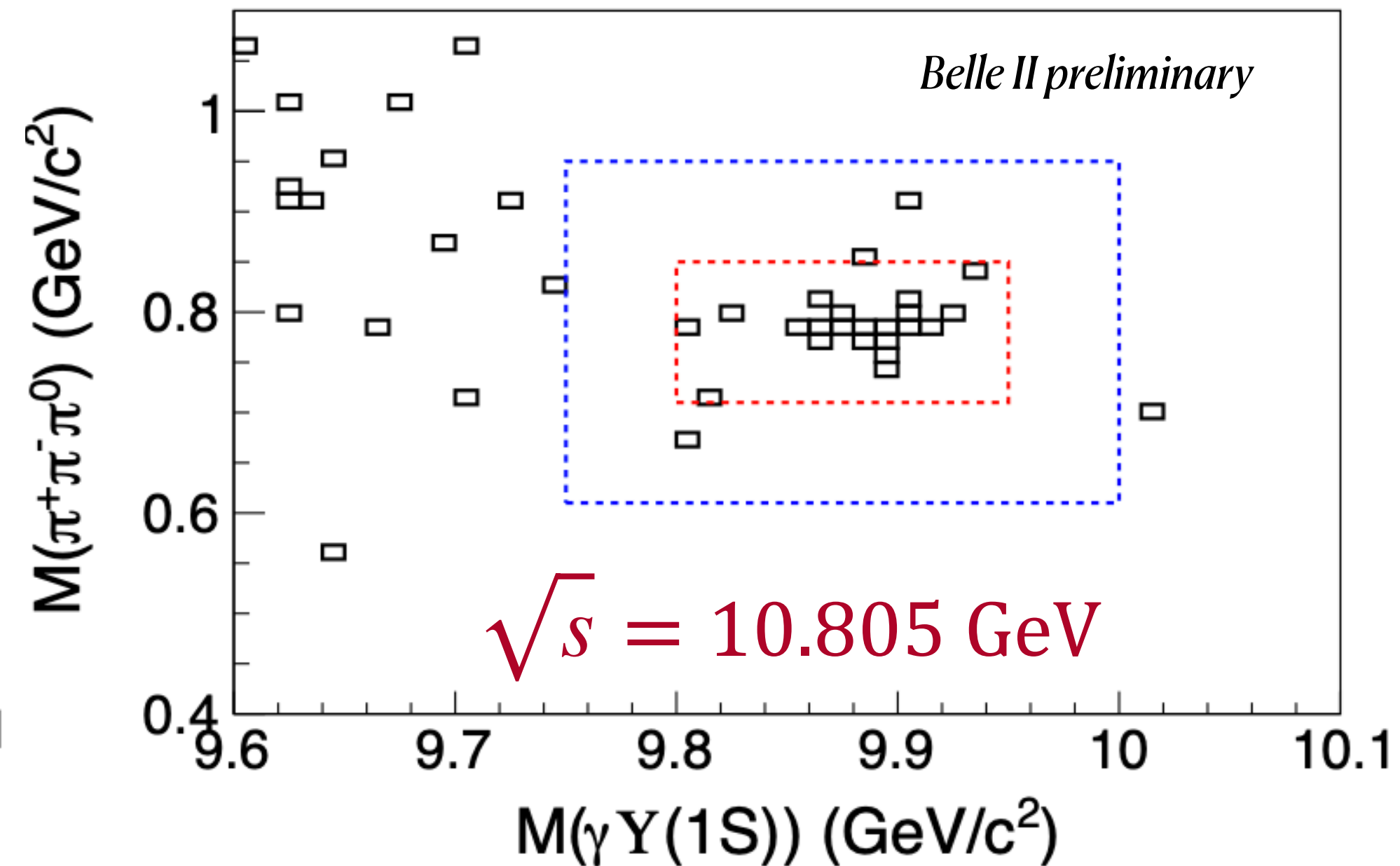
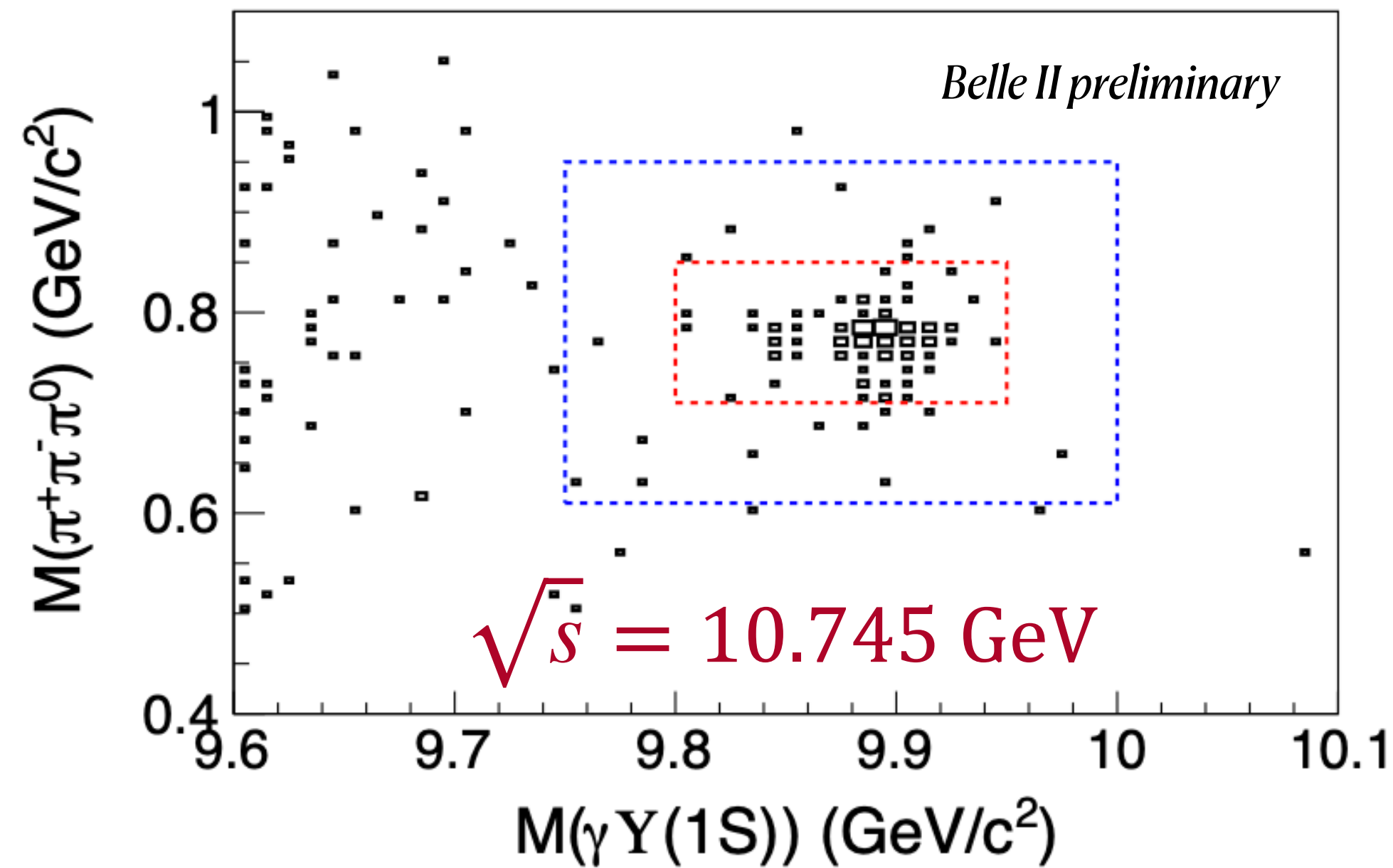


## • Event selection

- 4 or 5 charged tracks.
- standard Belle II PID: 90%-95% efficiency with 1-5% misID.
- photons from  $\chi_{bJ}$  decays:  $E_\gamma > 50$  MeV
- $\pi^0$  candidates:  $M(\gamma\gamma) \in (0.105, 0.150)$   $\text{GeV}/c^2$  with 90% efficiency.
- Constrained kinematic fit to  $\pi^+\pi^-\pi^0\gamma e^+e^-/\mu^+\mu^-$  final.
- Best candidate based on best fit quality.

## • Data driven corrections and systematics from control samples

# Mass distributions

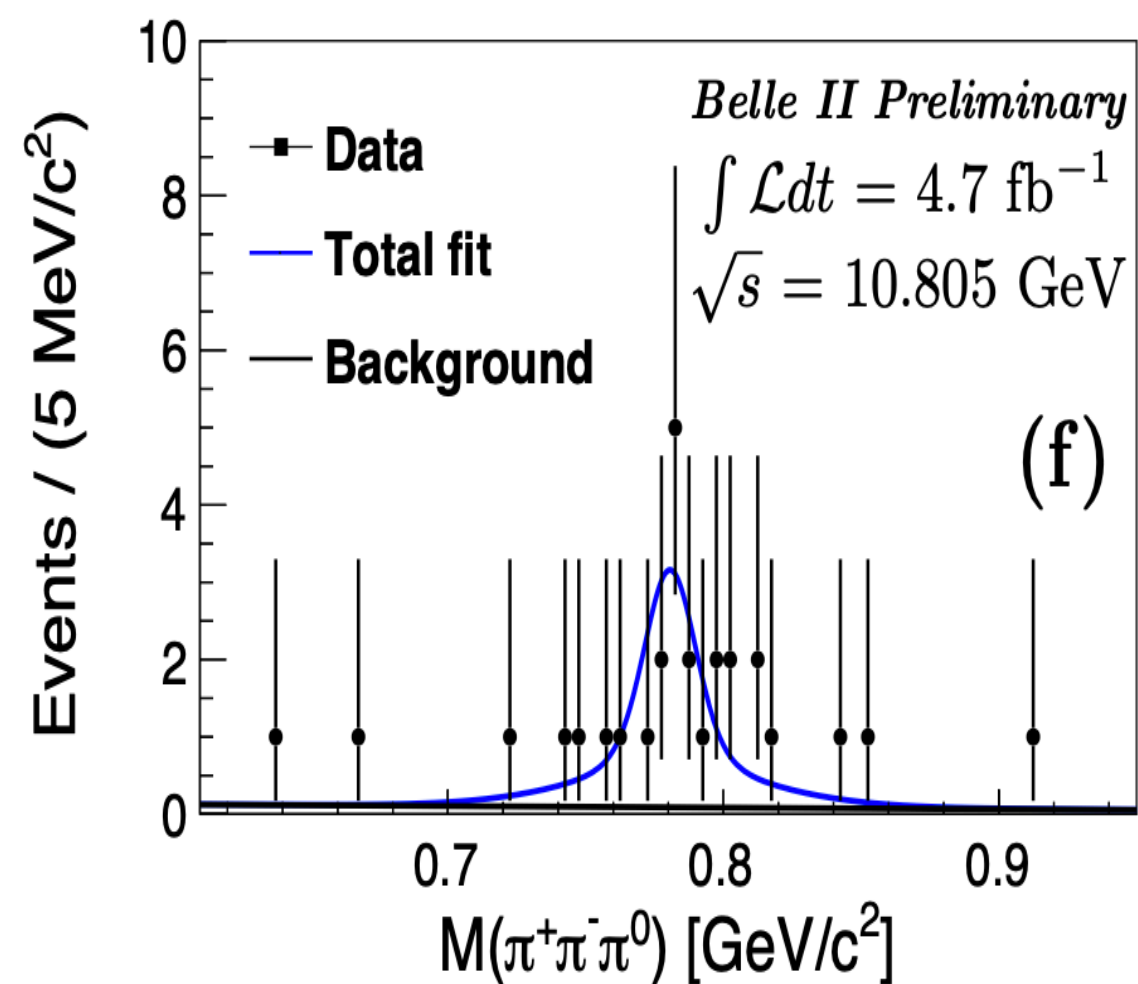
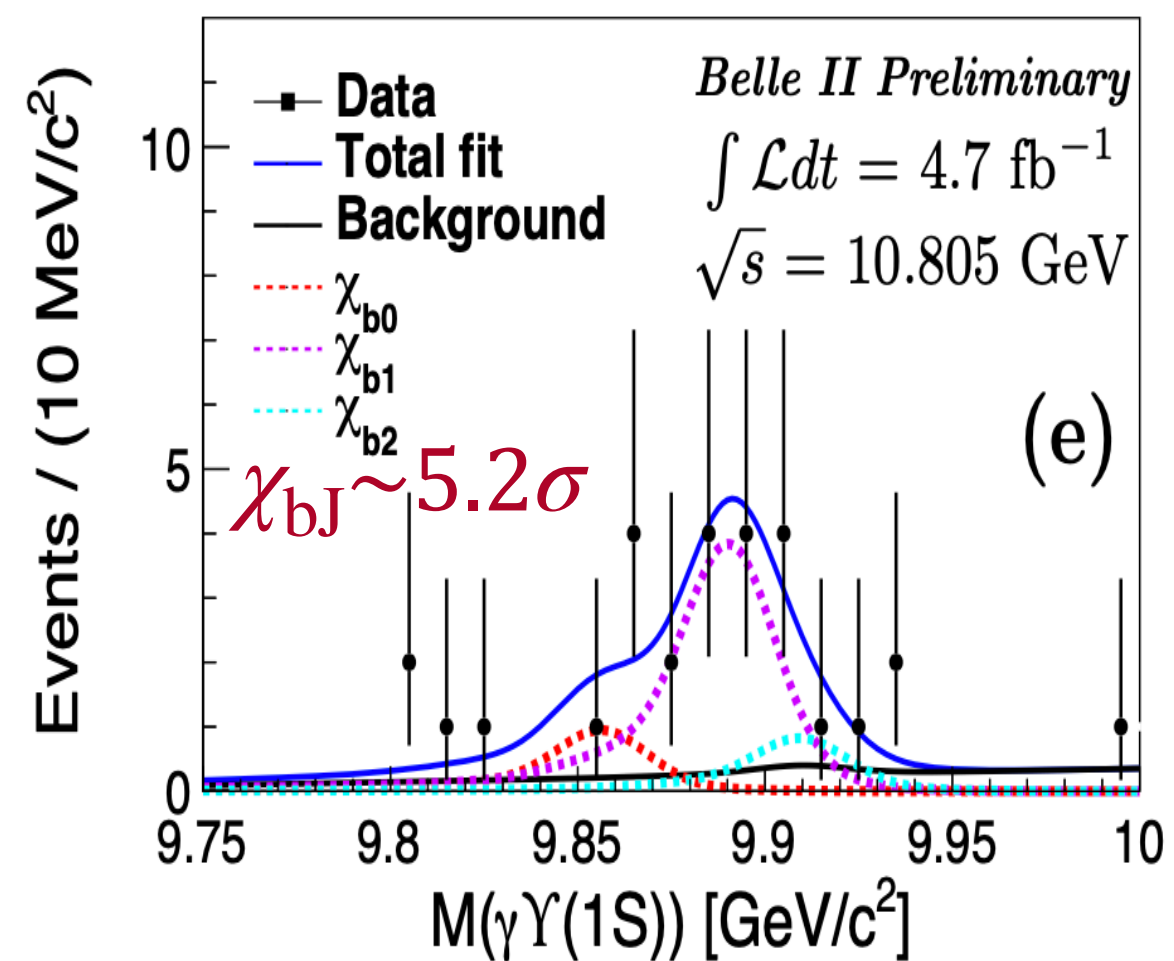
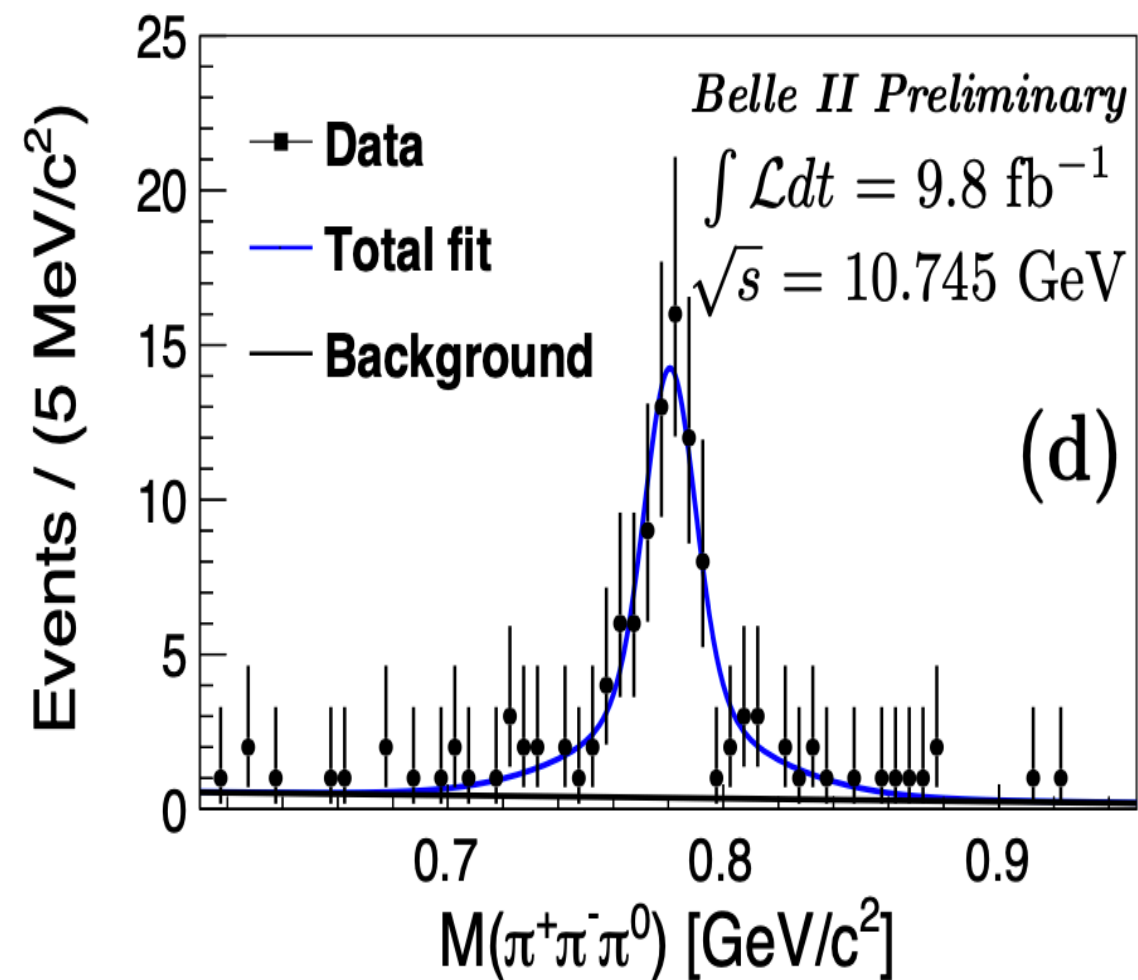
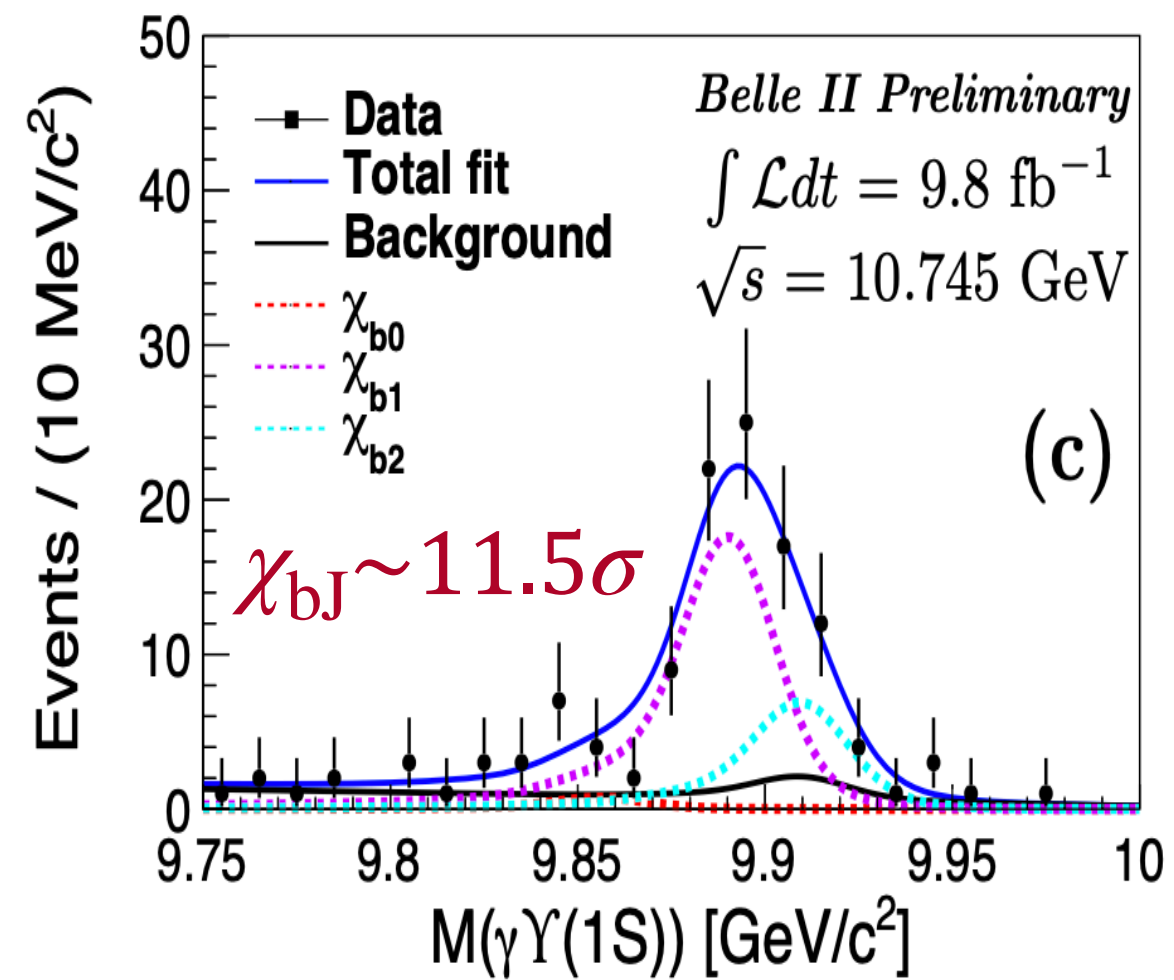


- Red box contains 95% of signals
- Blue box defines one-dimensional projection ranges



# Observation of $e^+e^- \rightarrow \omega\chi_{bJ}$

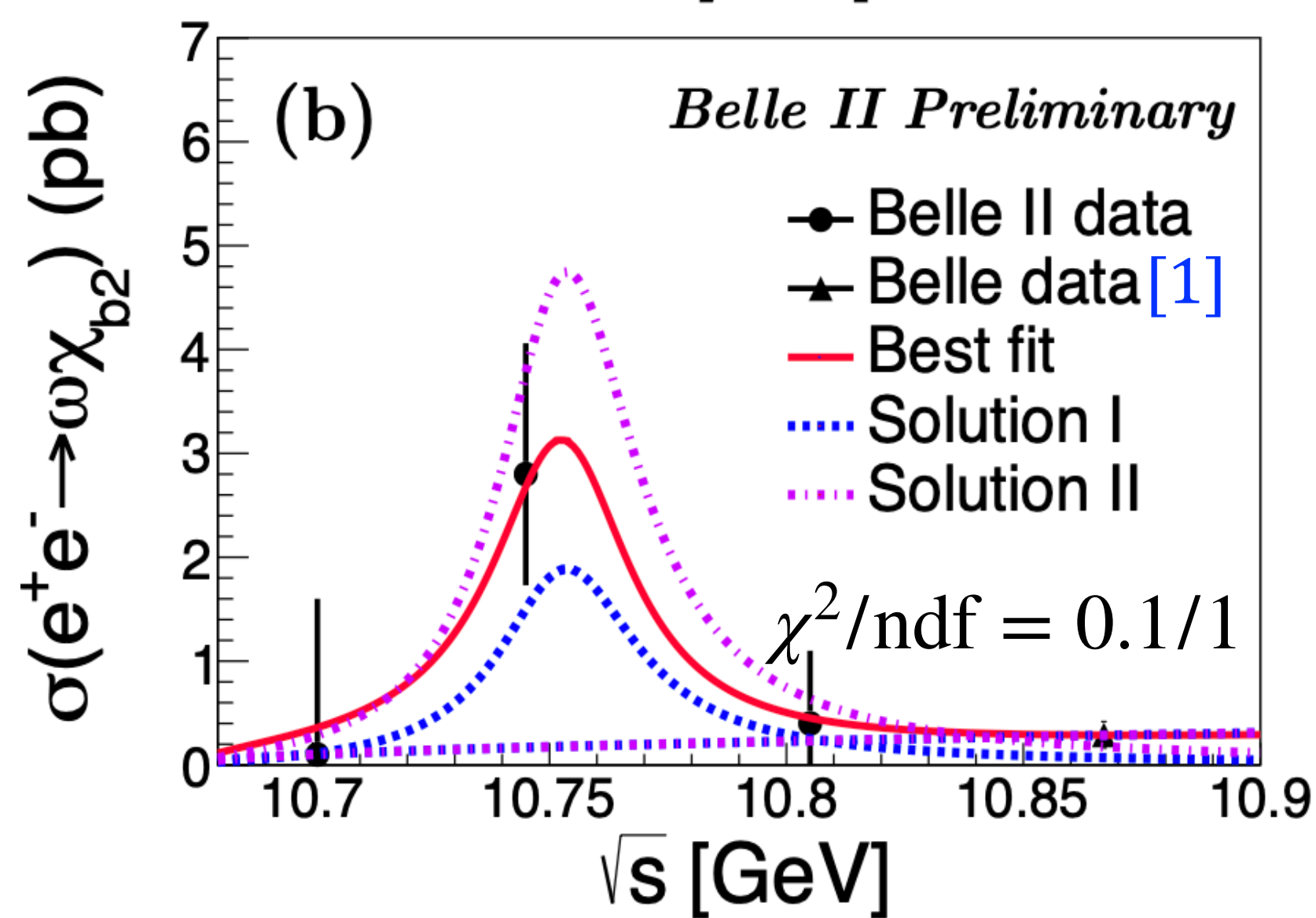
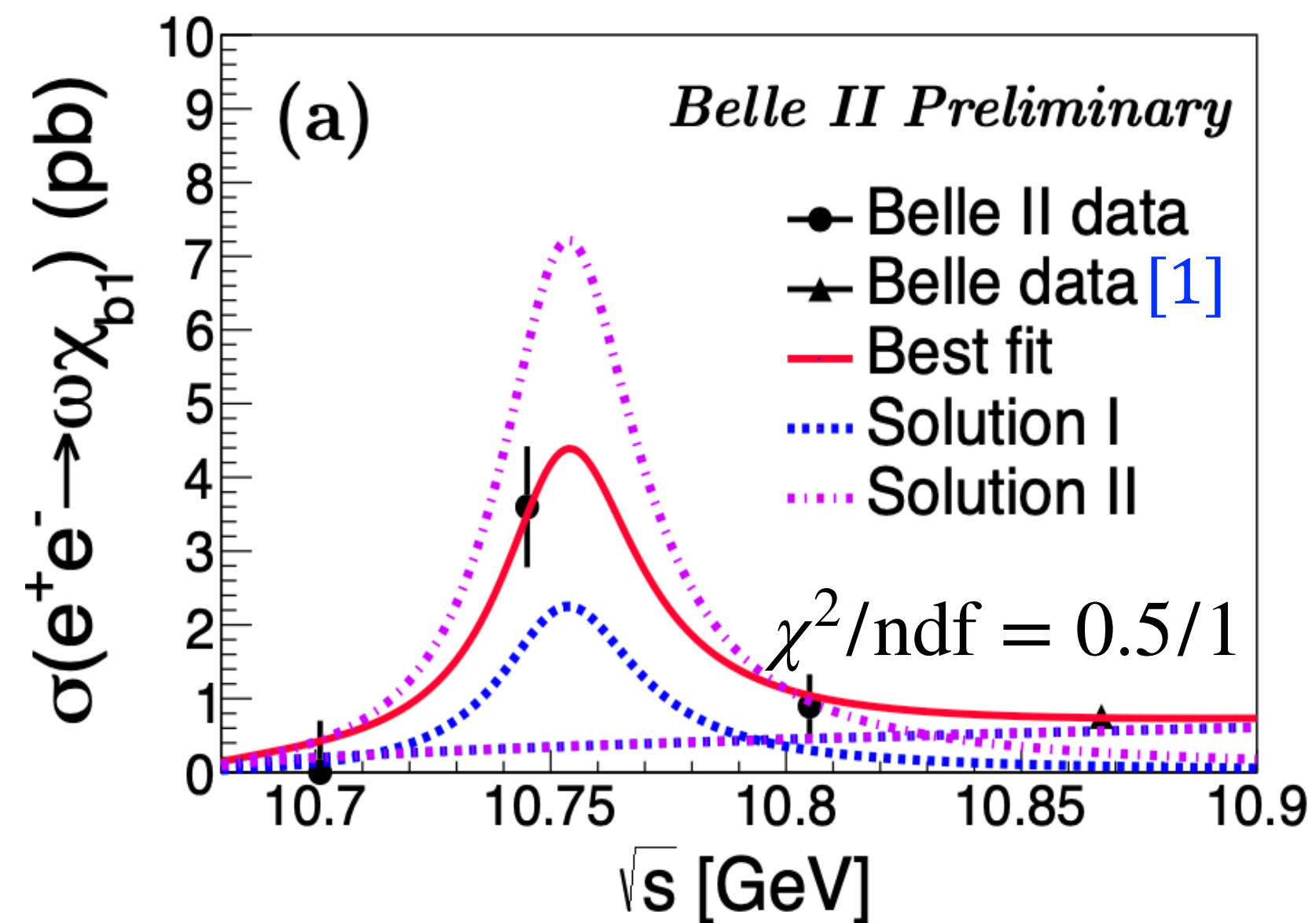
Two dimensional unbinned maximum likelihood fit to  $M(\gamma\Upsilon(1S))$  and  $M(\pi^+\pi^-\pi^0)$ .



| Channel                              | $\sqrt{s}$ (GeV) | $N^{\text{sig.}}$      | $\sigma_B^{(\text{up})}$ (pb)                 |
|--------------------------------------|------------------|------------------------|---|
| $e^+e^- \rightarrow \omega\chi_{b1}$ | 10.745           | $68.9^{+13.7}_{-13.5}$ | $3.6^{+0.7}_{-0.7}$ (stat.) $\pm 0.4$ (syst.) |
| $e^+e^- \rightarrow \omega\chi_{b2}$ |                  | $27.6^{+11.6}_{-10.0}$ | $2.8^{+1.2}_{-1.0}$ (stat.) $\pm 0.5$ (syst.) |
| $e^+e^- \rightarrow \omega\chi_{b1}$ | 10.805           | $15.0^{+6.8}_{-6.2}$   | 1.6 @ 90% C.L.                                |
| $e^+e^- \rightarrow \omega\chi_{b2}$ |                  | $3.3^{+5.3}_{-3.8}$    | 1.5 @ 90% C.L.                                |

*No evident signal are found at  $\sqrt{s} = 10.710 \text{ GeV}$ .*

# Observation of $\Upsilon(10753) \rightarrow \omega\chi_{bJ}$



The  $e^+e^- \rightarrow \omega\chi_{b1/2}$  cross sections peak at  $\Upsilon(10753)$  while no obvious peak at  $\Upsilon(10860)$  is found!

Combine with Belle measurement<sup>[1]</sup> to fit cross section with function:

$$\sigma_{\omega\chi_{b1/2}}(\sqrt{s}) = |\sqrt{PS_2(\sqrt{s}) + BW(\sqrt{s})e^{i\phi}}|^2, \quad BW(\sqrt{s}) = \frac{\sqrt{12\pi\Gamma_{ee}\mathcal{B}_f\Gamma}}{s - M^2 - iM\Gamma} \sqrt{\frac{PS_2(\sqrt{s})}{PS_2(M)}}$$

$M$  and  $\Gamma$  are fixed referring to Ref. [2]

| $\Gamma_{ee}\mathcal{B}_f$  | Solution I                    | Solution II                   |
|---|-------------------------------|-------------------------------|
| $\Gamma_{ee}\mathcal{B}(\Upsilon(10753) \rightarrow \omega\chi_{b1})$ | $(0.63 \pm 0.39 \pm 0.20)$ eV | $(2.01 \pm 0.38 \pm 0.76)$ eV |
| $\Gamma_{ee}\mathcal{B}(\Upsilon(10753) \rightarrow \omega\chi_{b2})$ | $(0.53 \pm 0.46 \pm 0.15)$ eV | $(1.32 \pm 0.44 \pm 0.55)$ eV |

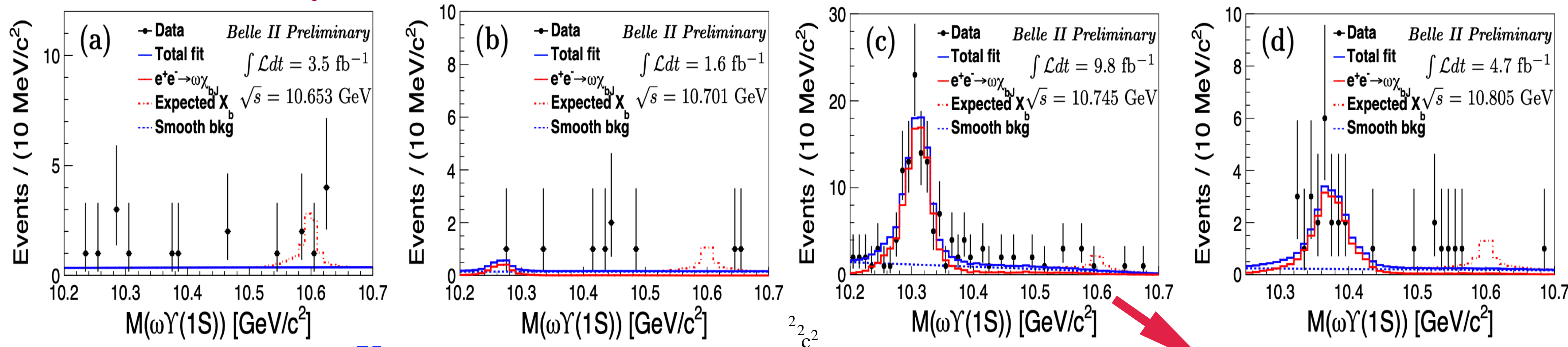
- $\frac{\Gamma_{ee}\mathcal{B}(\Upsilon(10753) \rightarrow \omega\chi_{b1})}{\Gamma_{ee}\mathcal{B}(\Upsilon(10753) \rightarrow \omega\chi_{b2})} \sim 1.0$  agrees with the expectation for NRQCD<sup>[3]</sup>
- $\frac{\Gamma_{ee}\mathcal{B}(\omega\chi_{b1/2})}{\Gamma_{ee}\mathcal{B}(\pi^+\pi^-\Upsilon(2S))}$ <sup>[2]</sup>  $\sim 1.5$  for  $\Upsilon(10753)$  and  $\sim 0.1$  for  $\Upsilon(10860)$

[1]PRL 113, 142001(2014); [2]. JHEP 10, 220(2019); [3]. arXiv:2112.09092;



# Search for $X_b$

$$e^+e^- \rightarrow \gamma X_b:$$



- No significant  $X_b$  signal is observed.
- The peaks are the reflections of  $e^+e^- \rightarrow \omega\chi_{bJ}$

From simulated events with  $M(X_b) = 10.6 \text{ GeV}/c^2$   
 The yield is fixed at the upper limit on 90% C.L.

| Upper limits of   | $\sqrt{s}$ (GeV)                          | 10.653       | 10.701       | 10.745       | 10.805       |
|---|---|--------------|--------------|--------------|--------------|
| $\sigma_B(e^+e^- \rightarrow \gamma X_b) \cdot \mathcal{B}(X_b \rightarrow \omega\Upsilon(1S))$ | $M(X_b) = 10.6 \text{ MeV}/c^2$           | 0.45         | 0.33         | 0.10         | 0.14         |
| (pb) at 90% C.L.  | $M(X_b) = (10.45, 10.65) \text{ MeV}/c^2$ | (0.14, 0.54) | (0.25, 0.84) | (0.06, 0.14) | (0.08, 0.36) |

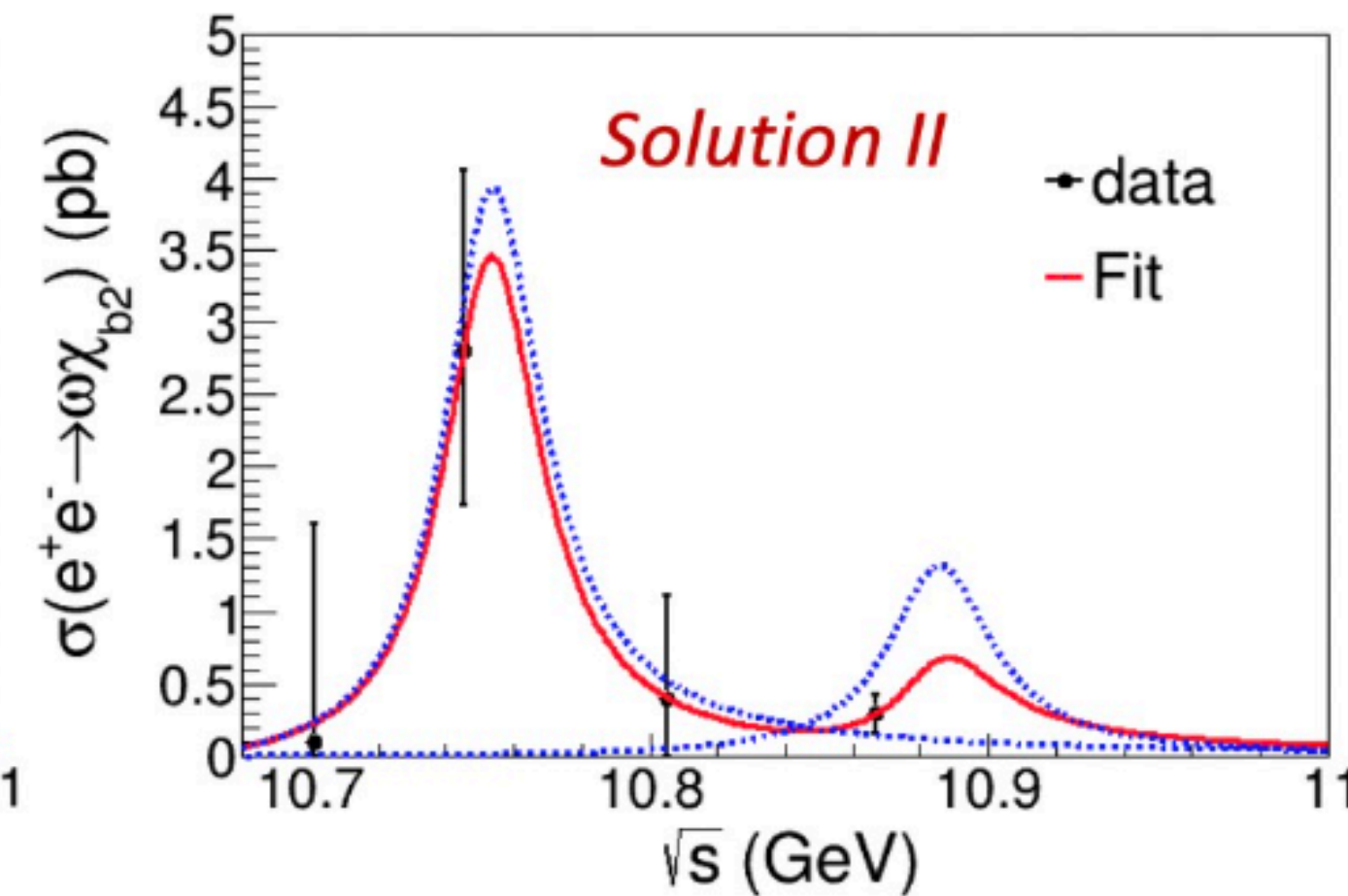
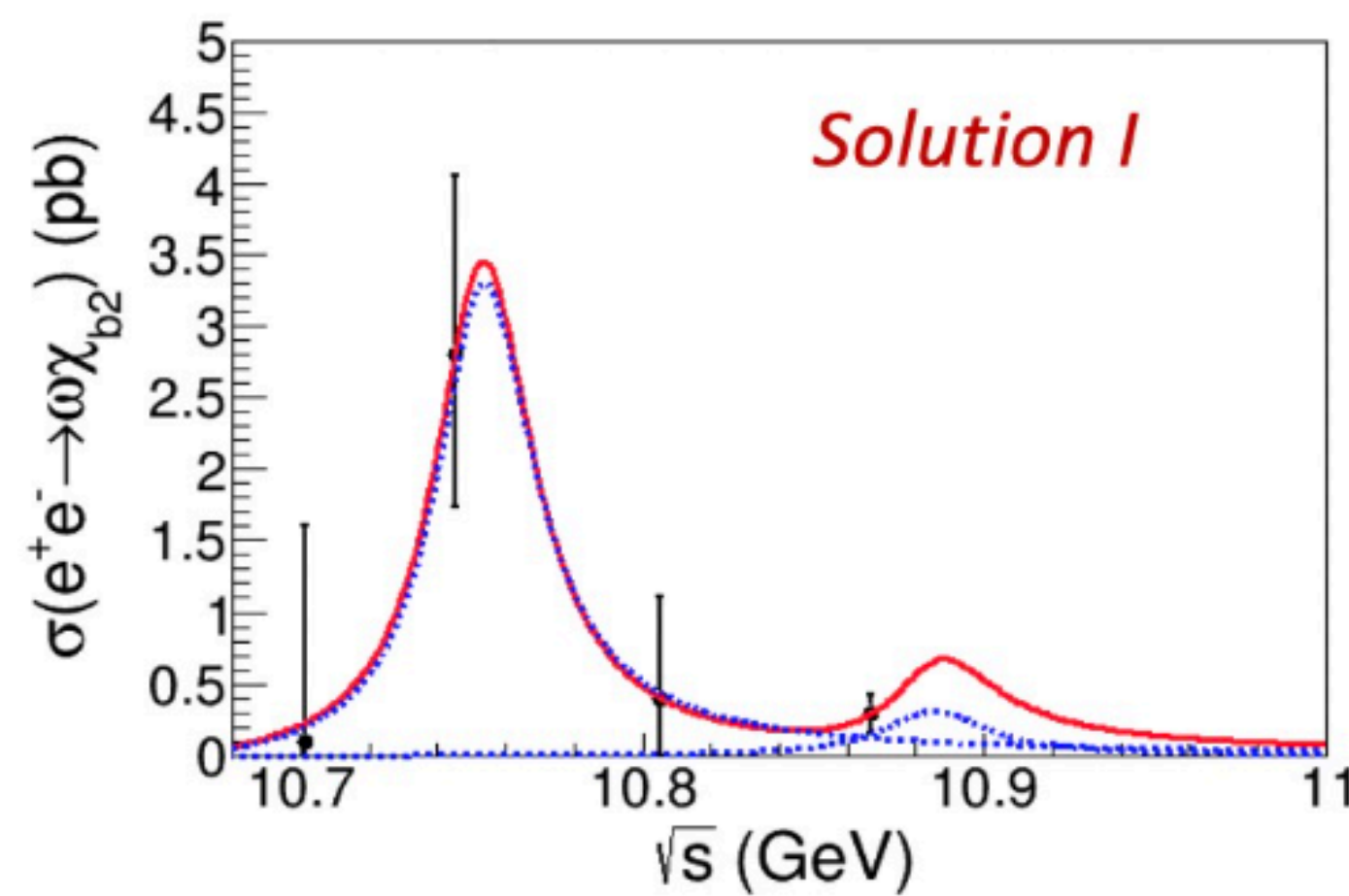
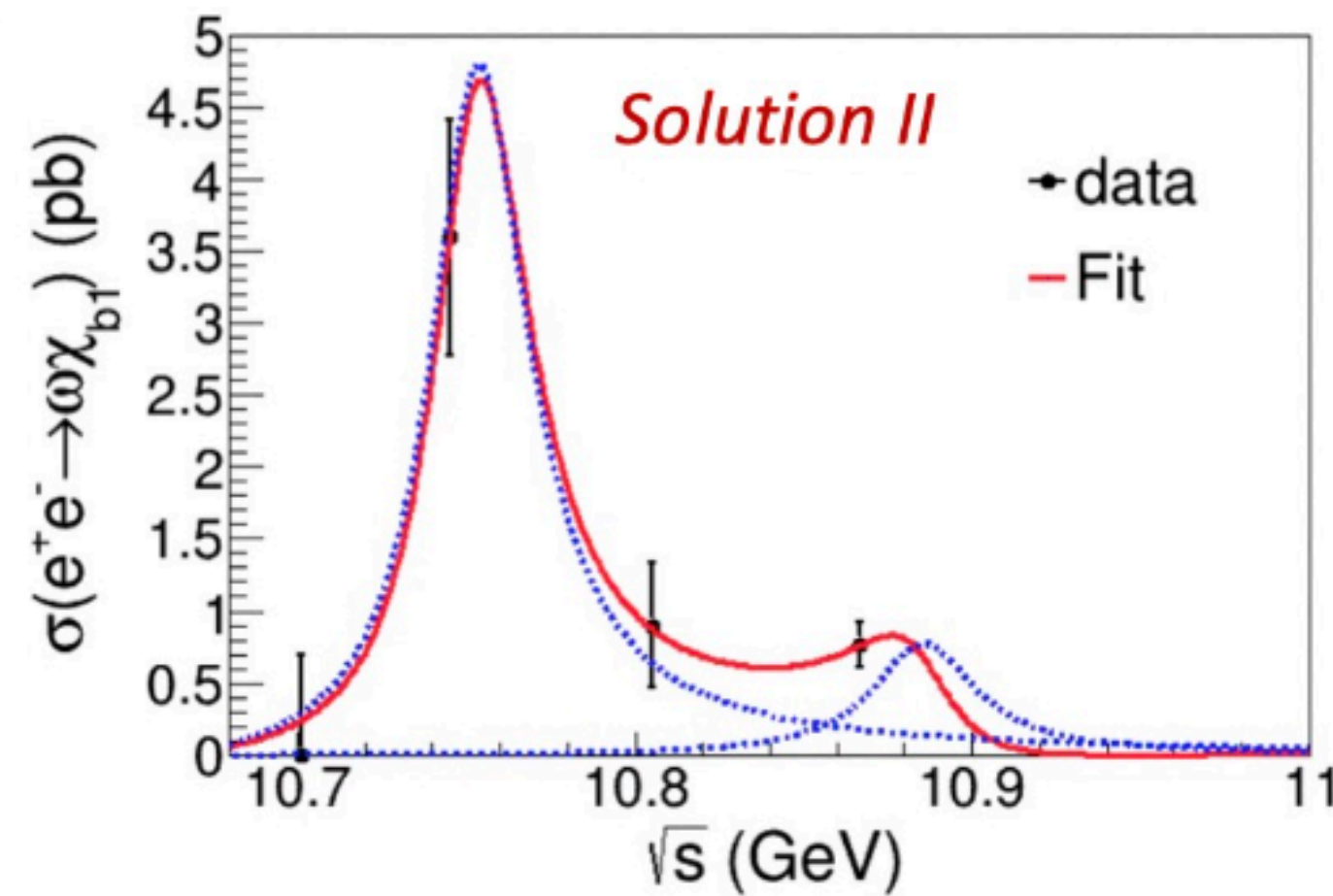
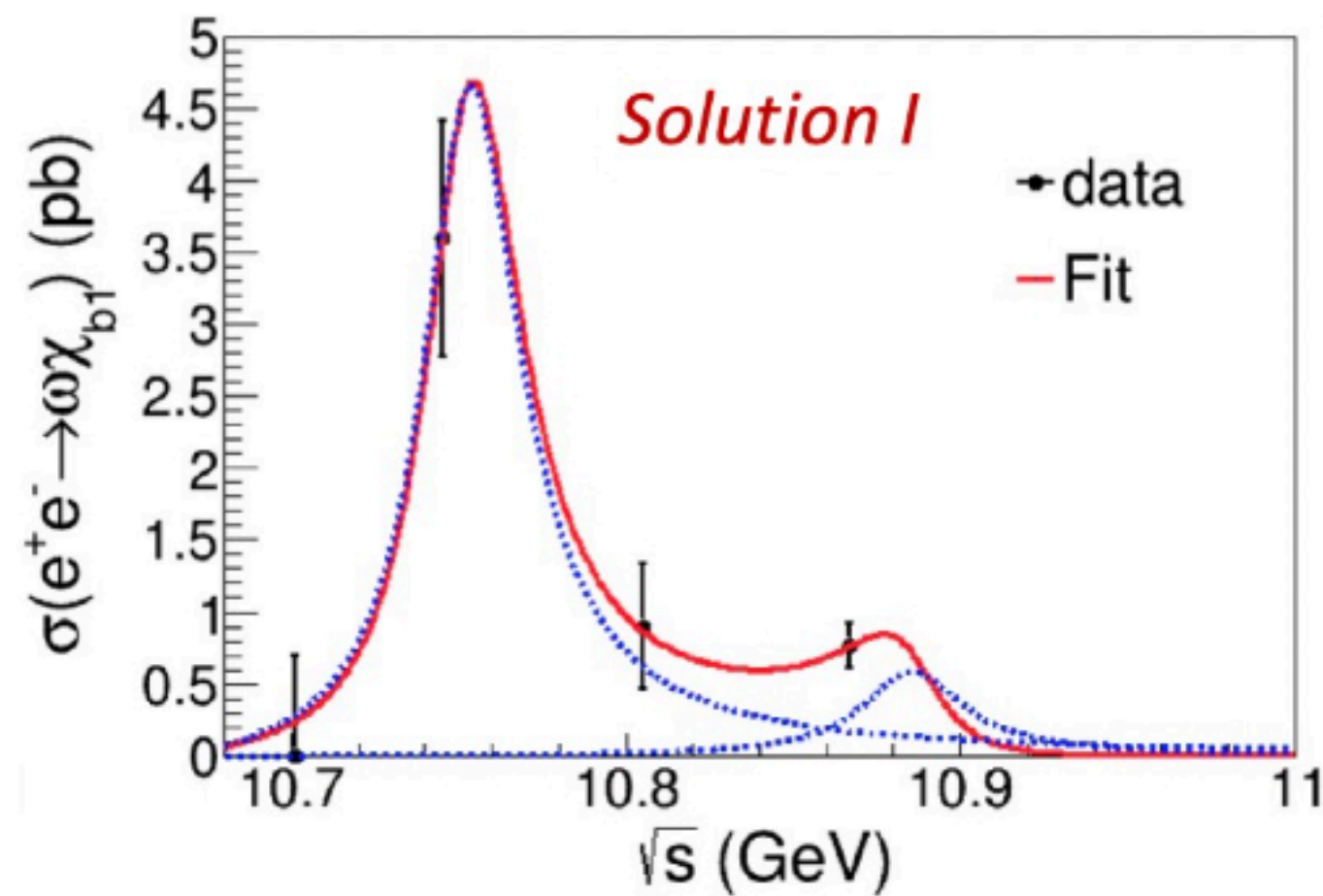
# Summary

- We are at the beginning of a long program of quarkonium physics.
- The unique scan data near  $\sqrt{s} = 10.75$  GeV at Belle II provide an opportunity to understand the nature of the  $\Upsilon(10753)$  energy region, as well as the quarkonium spectroscopy.
- New decay modes of  $\Upsilon(10753) \rightarrow \omega\chi_{bJ}$  are observed for the first time.
- No significant  $X_b$  signal is observed with a mass around  $10.6$  GeV/ $c^2$ , and the upper limits at 90% C.L. are set.
- Other active ongoing analyses based on unique scan data.



# Backup

# Alternative fit for $\sigma(e^+e^- \rightarrow \omega\chi_{bJ})$



$$\sigma_{\omega\chi_{c1/2}}(\sqrt{s}) = |BW_{\Upsilon(10753)} + BW_{\Upsilon(10806)}e^{i\phi}|^2$$

$M$  and  $\Gamma$  are fixed referring to Ref. [1][2]

$$\frac{\Gamma_{ee}B(\Upsilon(10753) \rightarrow \omega\chi_{b1})}{\Gamma_{ee}B(\Upsilon(10753) \rightarrow \omega\chi_{b2})}$$

**Solution I:**  $\frac{1.24 \pm 0.56(\text{stat.})}{0.92 \pm 0.37(\text{stat.})}$

**Solution II:**  $\frac{1.28 \pm 0.57(\text{stat.})}{1.09 \pm 0.40(\text{stat.})}$

$\chi^2/\text{ndf} = 0.4$  and  $0.1$  for  $\omega\chi_{b1}$  and  $\omega\chi_{b2}$

Ref: [1]. JHEP 10, 220(2019);

[2]. PDG 2022

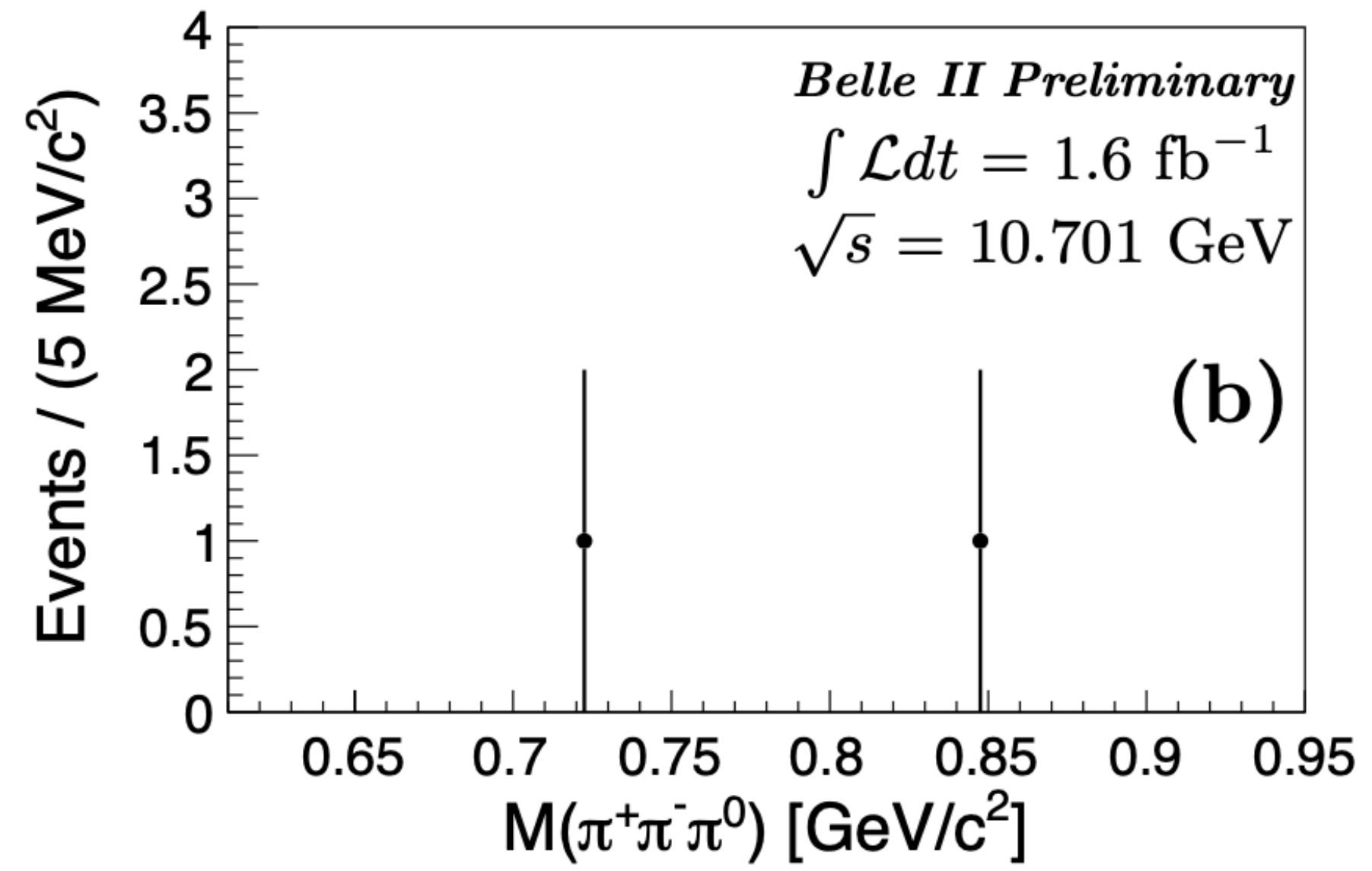
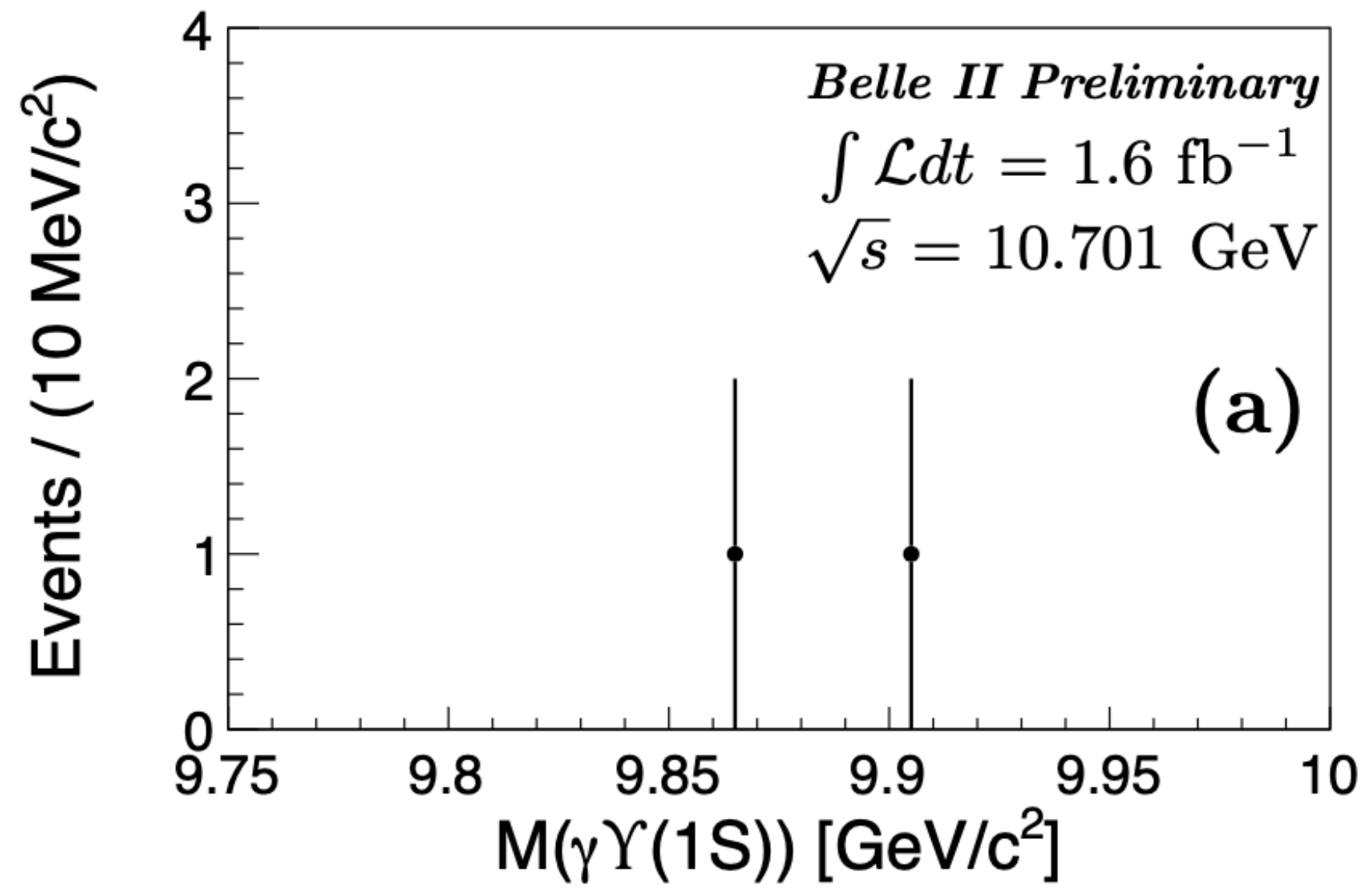
| Channel                              | $\sqrt{s}$ (GeV) | $N^{\text{sig}}$       | $N^{\text{UL}}$ | $\Sigma(\sigma)$ | $\varepsilon$ | $ 1 - \Pi ^2$ | $1 + \delta_{\text{ISR}}$ | $\sigma_{\text{syst}}(\%)$ | $\sigma^B$ (pb)   | $\sigma_B^{\text{UL}}$ (pb) |
|--------------------------------------|------------------|------------------------|-----------------|------------------|---------------|---------------|---------------------------|----------------------------|---|-----------------------------|
| $e^+e^- \rightarrow \omega\chi_{b0}$ | 10.701           | -                      | 3.0             | -                | 0.184         | 0.931         | 0.67                      | 15.7                       | -   | 16.5                        |
| $e^+e^- \rightarrow \omega\chi_{b1}$ |                  | $0.0^{+2.1}_{-0.0}$    | 3.9             | -                | 0.186         | 0.931         | 0.64                      | 9.2                        | $0.0^{+0.7}_{-0.0}(\text{stat.})$                       | 1.2                         |
| $e^+e^- \rightarrow \omega\chi_{b2}$ |                  | $0.1^{+2.2}_{-0.1}$    | 4.0             | -                | 0.184         | 0.931         | 0.62                      | 9.1                        | $0.1^{+1.4}_{-0.1}(\text{stat.})$                       | 2.5                         |
| $e^+e^- \rightarrow \omega\chi_{b0}$ | 10.745           | $3.0^{+5.5}_{-4.7}$    | 11.8            | 0.5              | 0.185         | 0.931         | 0.65                      | 17.0                       | $2.8^{+5.1}_{-4.4}(\text{stat.})$                       | 11.1                        |
| $e^+e^- \rightarrow \omega\chi_{b1}$ |                  | $68.9^{+13.7}_{-13.5}$ | -               | 5.9              | 0.185         | 0.931         | 0.65                      | 11.6                       | $3.6^{+0.7}_{-0.7}(\text{stat.}) \pm 0.4(\text{syst.})$ | -                           |
| $e^+e^- \rightarrow \omega\chi_{b2}$ |                  | $27.6^{+11.6}_{-10.0}$ | -               | 3.1              | 0.186         | 0.931         | 0.65                      | 13.5                       | $2.8^{+1.2}_{-1.0}(\text{stat.}) \pm 0.5(\text{syst.})$ | -                           |
| $e^+e^- \rightarrow \omega\chi_{b0}$ | 10.805           | $3.6^{+3.8}_{-3.1}$    | 9.8             | 1.2              | 0.184         | 0.932         | 1.12                      | 21.1                       | $4.1^{+4.3}_{-3.5}(\text{stat.})$                       | 11.2                        |
| $e^+e^- \rightarrow \omega\chi_{b1}$ |                  | $15.0^{+6.8}_{-6.2}$   | 26.0            | 2.7              | 0.184         | 0.932         | 1.12                      | 16.6                       | $0.9^{+0.4}_{-0.4}(\text{stat.})$                       | 1.6                         |
| $e^+e^- \rightarrow \omega\chi_{b2}$ |                  | $3.3^{+5.3}_{-3.8}$    | 12.5            | 0.8              | 0.185         | 0.932         | 1.11                      | 16.8                       | $0.4^{+0.7}_{-0.5}(\text{stat.})$                       | 1.5                         |



# Systematic uncertainty(%) on $\sigma^B(e^+e^- \rightarrow \omega\chi_{bJ})$

and  $\sigma_B^{UL}(e^+e^- \rightarrow \gamma X_b) \times \mathcal{B}(X_b \rightarrow \omega Y(1S))$

| Final states                | $\omega\chi_{b0}/\omega\chi_{b1}/\omega\chi_{b2}$ |                |                |        | $\gamma X_b$ |        |        |        |
|-----------------------------|---|----------------|----------------|--------|--------------|--------|--------|--------|
|                             | $\sqrt{s}$ (GeV)                                  | 10.701         | 10.745         | 10.805 | 10.653       | 10.701 | 10.745 | 10.805 |
| Detection efficiency        | 4.9   | 4.9            | 4.9            | 4.9    | 4.9          | 4.9    | 4.9    | 4.9    |
| Branching fractions         | 14.7/7.4/7.3                                      | 14.7/7.4/7.3   | 14.7/7.4/7.3   | 4.7    | 4.7          | 4.7    | 4.7    | 4.7    |
| Radiative correction factor | 2.0   | 5.1            | 13.7           | 0.2    | 0.4          | 0.5    | 0.7    |        |
| Angular distribution        | 1.0   | 1.0            | 1.0            | 1.0    | 1.0          | 1.0    | 1.0    | 1.0    |
| Fit model                   | 1.0   | 3.3/4.6/8.2    | 2.1/1.6/1.0    | 8.6    | 3.2          | 7.0    | 7.7    |        |
| Trigger                     | 1.0   | 1.0            | 1.0            | 1.0    | 1.0          | 1.0    | 1.0    | 1.0    |
| Beam-energy                 | -   | 3.2/2.5/3.0    | 3.5/2.3/3.6    | -      | -            | -      | -      |        |
| Luminosity                  | 0.6   | 0.6            | 0.6            | 0.6    | 0.6          | 0.6    | 0.6    | 0.6    |
| Sum                         | 15.7/9.2/9.1                                      | 17.0/11.6/13.5 | 21.1/16.6/16.8 | 11.1   | 7.7          | 9.9    | 10.4   |        |





# Belle II potential — 10.75 GeV

Other active ongoing analyses based on unique scan data:

| Channel                                     |
|---|
| $B\bar{B}$ decomposition                    |
| $e^+e^- \rightarrow \omega\eta_b(1S)$       |
| $e^+e^- \rightarrow \phi\eta_b(1S)$         |
| $e^+e^- \rightarrow \eta h_b(1P)$           |
| $e^+e^- \rightarrow \Upsilon(1S) + X$       |
| $e^+e^- \rightarrow \pi^+\pi^-Y_2(1D)$      |
| $e^+e^- \rightarrow \pi^+\pi^-\Upsilon(nS)$ |
| $e^+e^- \rightarrow \pi^+\pi^-h_b(nP)$      |

- Precise measurements of the mass and width of  $\Upsilon(10753)$
- Search for more decays of  $\Upsilon(10753)$
- Search for the the  $X_b$  state (the bottomonium counterpart of  $X(3872)$ )
- Study the  $\pi^+\pi^-/\omega/\eta/\phi$  transitions in the  $e^+e^-$  annihilations to test NRQCD